CHAPTER 7

Ozone and Stratospheric Chemistry

LEAD AUTHOR

M. R. Schoeberl

CONTRIBUTING AUTHORS

A. R. Douglass
J. C. Gille
J. A. Gleason
W. R. Grose
C. H. Jackman
S. T. Massie
M. P. McCormick
A. J. Miller
P. A. Newman
L. R. Poole
R. B. Rood
G. J. Rottman
R. S. Stolarski
J. W. Waters

Chapter 7 Contents

7.1 Stratospheric ozone - background

7.1.1 Why is understanding stratospheric ozone important?

Ozone is one of the most important trace species in the atmosphere. Ozone plays two critical roles: it removes most of the biologically harmful ultraviolet light before the light reaches the surface, and it plays an essential role in setting up the temperature structure and therefore the radiative heating/cooling balance in the atmosphere, especially the stratosphere (the region between about 10 and 60 km).

FIGURE 7.1

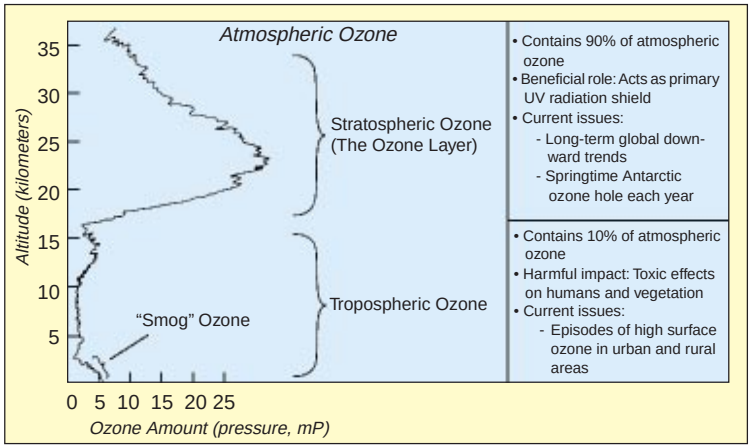

The distribution of atmospheric ozone in partial pressure as a function of altitude.

7.1.1.1 Location of the ozone layer and climatology

Ozone is mainly found in two regions of the atmosphere. Most of the ozone can be found in a layer between 10 and 60 km above the Earth's surface (Figure 7.1). This ozone region located in the stratosphere is known as the "ozone layer." Some ozone can also be found in the lower atmosphere (below 10 km) in the region known as the troposphere. Although chemically identical to stratospheric ozone, tropospheric ozone is quite distinct and geophysically different from stratospheric ozone, and the science issues concerning tropospheric ozone are discussed in Chapter 4.

7.1.1.2 Ozone and UV—biological threat

Ozone is produced by the photolysis of molecular oxygen, O_2. The oxygen atom, O, produced by this photolysis recombines with O_2 to form ozone, O_3. Ozone formation primarily occurs in the tropical upper stratosphere, where it is transported poleward and downward by the large-scale Brewer-Dobson circulation. The global distribution of total ozone is shown in Figure 7.2 (pg. 312). This figure represents the 13-year average of the total ozone measurements taken by the Nimbus-7 Total Ozone Mapping Spectrometer (TOMS) instrument.

The formation of ozone by the photolysis of molecular oxygen removes most of the incident sunlight with wavelengths shorter than 200 nm. The wavelengths between 200 and 310 nm are removed by the photolysis of ozone itself. This photolysis of ozone in the stratosphere is the process by which most of the biologically damaging ultraviolet sunlight (UV-B) is filtered out.

As this filtering process occurs, the stratosphere is heated. This heating is responsible for the temperature structure of the stratosphere, where the temperature increases as the altitude increases. Without this filtering, larger amounts of UV-B would reach the surface. Numerous studies have shown that excessive exposure to UV-B is harmful to plants, animals, and humans (WMO 1992).

7.1.1.3 Ozone and climate change

If ozone in the stratosphere were to be removed, the stratosphere would cool. How a cooler stratosphere affects radiative balance in the rest of the atmosphere has been the subject of many detailed studies. These studies have been reanalyzed and integrated into the latest Intergovernmental Panel on Climate Change (IPCC) report, "Climate Change 1994: Radiative Forcing of Climate Change" (1995). The conclusion of that report is that stratospheric ozone loss leads to a "small but non-negligible offset to the total greenhouse forcing from CO_2, N_2O, CH_4, CFCs...." It is ironic that the size of the negative radiative forcing from ozone loss is nearly equal to the positive radiative forcing from chlorofluorocarbons (CFCs), the source of the stratospheric ozone loss. The size of the radiative forcing due to stratospheric ozone loss has also been shown to be very sensitive to the profile shape assumed for that loss.

Figure 7.2

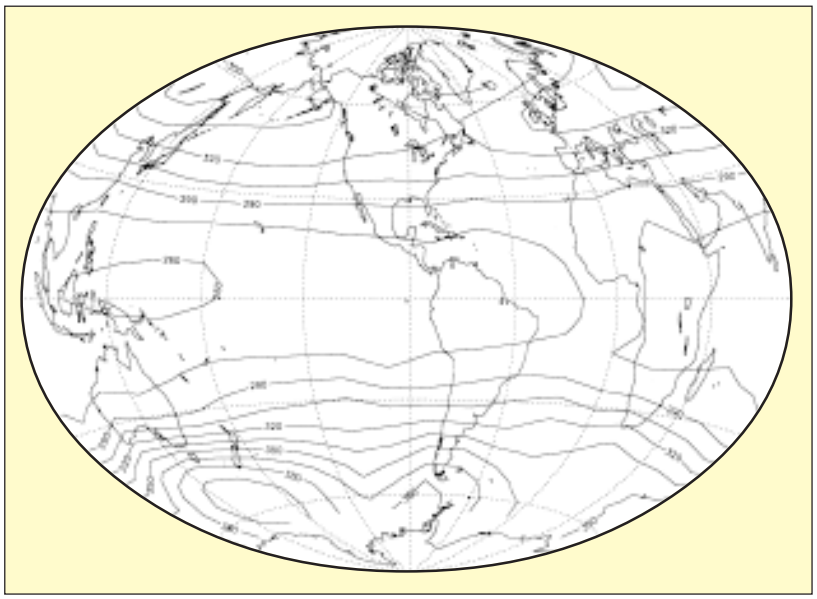

The global distribution of column or total ozone averaged over the 13 years of Nimbus-7 TOMS data in Dobson Units (DU).

7.1.2 Observed ozone changes

While the global amount of ozone is fairly constant, there are significant local, seasonal, and long-term changes. The causes of these changes are discussed in detail in Section 7.1.3.

The seasonal ozone changes are basically determined by the winter-summer changes in the stratospheric circulation. Since ozone has a lifetime of weeks to months in the lower stratosphere, the amount of ozone can strongly vary due to transport by stratospheric wind systems. Since weather conditions in the stratosphere, as in the troposphere, vary from year to year, there is also interannual variability in ozone amounts. Interseasonal changes in ozone are also linked to the 11-year solar cycle in UV output and the amount of volcanic aerosols in the stratosphere. Changes in ozone have also been linked to anthropogenic pollutants, especially the release of man-made chemicals containing chlorine. In the section below we describe the more-significant recent global changes in ozone observed by a variety of instruments.

7.1.2.1 Polar ozone changes

The first ozone measurements in the Antarctic were made during the 1950s. A Dobson instrument was installed at Halley Bay in late 1956 in preparation for the International Geophysical Year in 1957. One of the first discoveries made by this instrument was that the seasonal cycle of ozone in the south polar region is very different from that which had been observed in the north. This was noted in a review article by Dobson (1966), which pointed out that its cause was a difference in the circulation patterns of the Antarctic relative to the Arctic. In the Arctic, the total ozone amount grew rapidly in the late winter and early spring to about 500 Dobson Units (DU). (A DU is one milliatmosphere-cm of pure ozone; a layer of pure ozone that would be 0.001-cm thick under conditions of Standard Temperature and Pressure [STP].) In contrast, the Antarctic early springtime amounts remained near 300 DU.

The Dobson instrument at Halley Bay continued to make measurements each year. Farman et al. (1985) showed that the springtime ozone amounts over Halley Bay had declined from nearly 300 DU in the early 1960s to about 180 DU in the early-to-mid 1980s. This result has been confirmed at a number of other stations and shown using satellite data to occur over an area larger than the Antarctic continent (Stolarski et al. 1986). These large ozone changes implied that losses must be taking place in the lower stratosphere where most of the ozone exists. This was shown to be true in a series of ozonesonde measurements (see, e.g., Hofmann et al. 1989 and Figure 7.3). More-recent sonde measurements have shown instances of near-zero concentrations of ozone over a 5-km altitude range (Hofmann et al. 1994). Aircraft measurements (Proffitt et al. 1989) and satellite measurements (McCormick et al. 1988) confirm and show further details of these ozone changes.

The 1996-1997 Northern Hemisphere winter experienced a significant ozone depletion over the Arctic and subsequent total ozone values achieved record low values in the spring. Long term records of the Total Ozone Mapping Spectrometer (TOMS) (Newman et al., 1997) and ground based observations (Fioletov et al., 1997) show a downward change over the past several years occurring mostly in February and March and confined to the lower

FIGURE 7.3

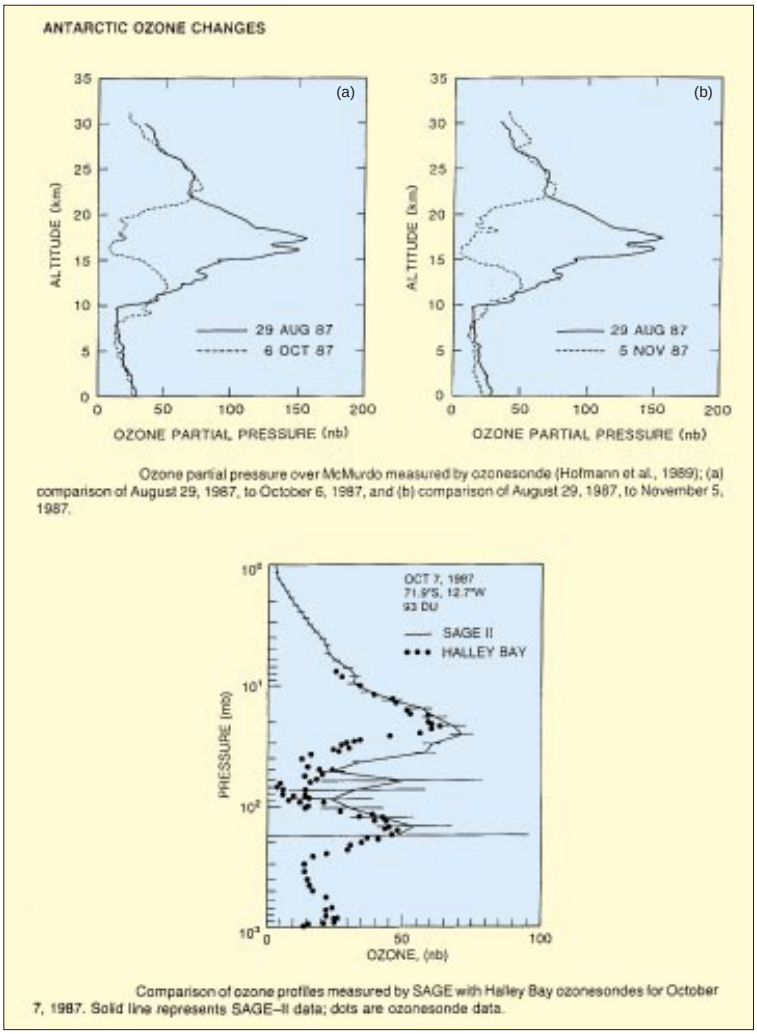

Balloonsonde ozone measurements made at McMurdo and SAGE II measurements for 1987.

stratosphere (Manney et al. 1997) similar to the depletion over the Antarctic. Total ozone changes for both polar regions are shown in Figure 7.4 (pg. 314) (Newman, Private communication). Chlorine radicals have been conclusively identified as the causes of ozone depletion now in both hemispheres. Measurements of ClO by the UARS MLS instrument (Santee et al., 1997) observed elevated levels in late February over Northern Hemisphere polar regions. The winter of 1996-1997, showed extremely low temperatures in the Stratosphere. These cold temperatures led to the formation of polar stratospheric clouds whose particles shift chlorine gas away from its HCl reservoir to active ClO through heterogeneous chemistry. This is the primary mechanism producing the Antarctic ozone hole (Anderson et al., 1991, Solomon, 1990, and others). Although the buildup of chlorine has occurred approximately uniformly in both hemisphere the unusually low temperatures reached in high northern latitudes mostly likely precipitated the concurrent ozone losses over the Arctic.

7.1.2.2 Midlatitude ozone loss

Midlatitude ozone loss estimates must be extracted from long time series using statistical models (see, e.g., Report of the International Ozone Trends Panel 1990). The longest time series of total ozone data is from Arosa in Switzerland. This time series, which dates back to 1926, is shown in Figure 7.5 (pg. 314). The Arosa data show a relatively constant amount of ozone for over 4 decades and a decrease in the last decade and a half. Analysis of a more-extensive network of 30+ stations which have been in operation for about 35 years shows negative trends over the last 1.5 decades, especially in the winter and early spring (see, e.g., Reinsel et al. 1994).

High-quality global satellite data records began in November 1978 with the launch of the Nimbus-7 Solar Backscatter Ultraviolet (SBUV) radiometer and TOMS instruments. These data show midlatitude trends in the Northern Hemisphere which are largest in the winter and early spring, peaking at about 6-8% per decade at 40˚-50° N in February (see, e.g., Randel and Cobb 1994; Hollandsworth et al. 1995). These satellite trends are in the process of being updated with a version 7 algorithm for the TOMS and SBUV instruments.

Changes in the profile of ozone with altitude can be deduced from sonde data or from the Stratospheric Aerosol and Gas Experiment (SAGE) satellite measurements. Analyses of sonde data (e.g., Logan 1994) show ozone decreases between the tropopause and about 24-km altitude. Analyses of SAGE data show larger decreases than those derived from sondes. SAGE results show negative ozone trends in the lower stratosphere in the tropics. Column ozone changes deduced from SBUV and TOMS show only small downward trends. Hollandsworth et al.

Figure 7.4

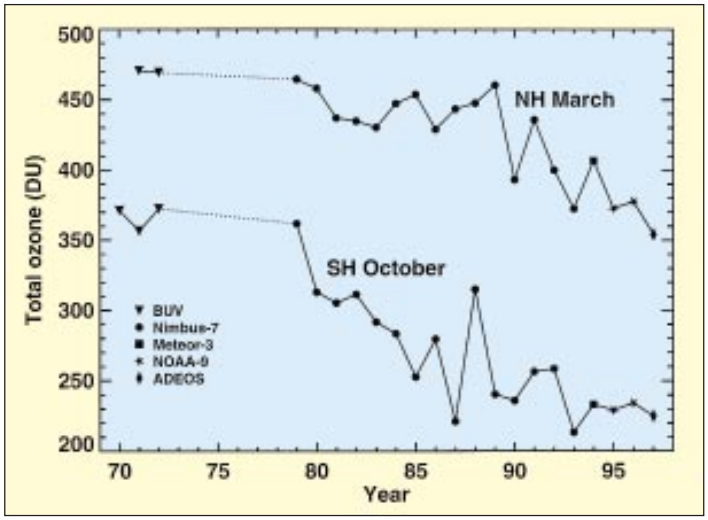

63˚ - 90˚ total ozone average

(1995) used SBUV profile and total ozone trends to deduce that ozone in the tropics below 32 hPa has increased slightly over the last decade. The resolution of the uncertainty in the magnitude of lower stratospheric and upper tropospheric ozone trends is an important measurement and analysis issue for the coming years.

Figure 7.5

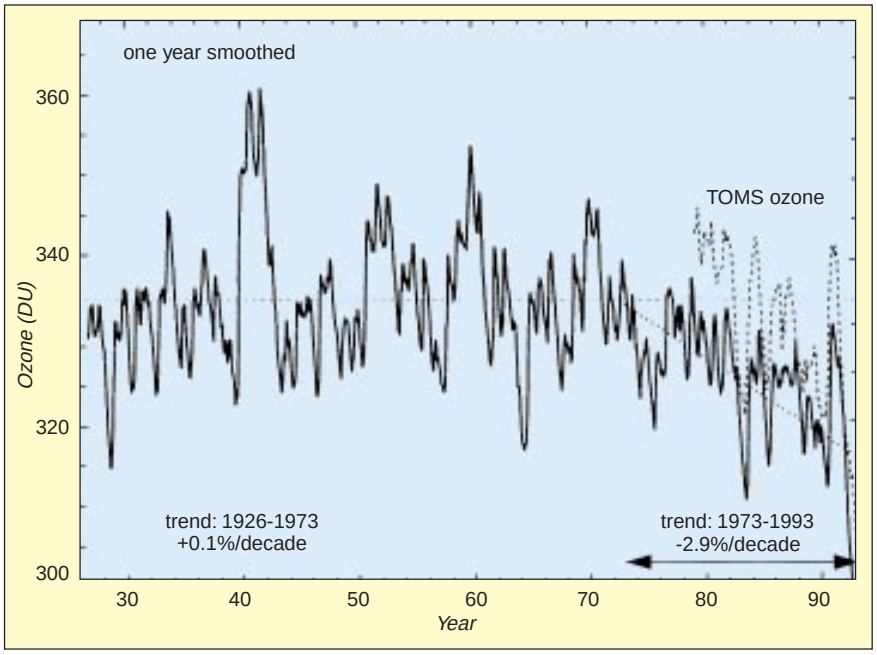

Time series of column ozone measurements at Arosa, Switzerland, in DU.

7.1.3 The stratospheric ozone distribution

7.1.3.1 Chemical processes

Ozone is being continuously created and destroyed by the action of ultraviolet sunlight. The overall amount of ozone in the global stratosphere is determined by the magnitude of the production and loss processes and by the rate at which air is transported from regions of net production to those of net loss.

Production of ozone requires the breaking of an O_2 bond, with the extra or "odd" oxygen atom attaching to another O_2 to form O_3. This most frequently occurs via the photodissociation of O_2 by solar ultraviolet radiation. In the lower stratosphere and troposphere ozone can also be produced by photochemical smog-like reactions. In these reactions H or CH_3 or higher hydrocarbon radicals attach to an O_2 forming HO_2 or CH_3O_2, etc., which then react with NO. This reaction breaks the O_2 bond by forming NO_2 (which is really ONO). When NO_2 is photolyzed an O atom is formed which reacts with O_2 to form O_3. Loss of ozone occurs when an O atom reacts with O_3 to re-form the O_2 bond. More importantly, this loss process is catalyzed by the oxides of hydrogen, nitrogen, chlorine, and bromine. These oxides are produced in the stratosphere from long-lived, unreactive molecules released at the surface of the Earth. The major source molecules for HO_x (HO_x is chemical shorthand for the sum of all the hydrogen radicals—OH and HO_2, mostly) are methane (CH_4) and water vapor (H_2O). The main source of NO_x (NO_x is chemical shorthand for the sum of all nitrogen radicals—NO, NO_2, N_2O_5, NO_3, mostly) is nitrous oxide (N_2O). The major sources of chlorine are industrially-produced CFCs (such as CFC-11, which is $CFCl_3$, and CFC-12, which is CF_2Cl_2) and naturally-occurring methyl chloride (CH_3Cl). The major

sources of bromine are methyl bromide (CH_3Br) and the halons (CF_3Br and CF_2ClBr). These source molecules are transported to the stratosphere where they react or are photodissociated to produce the catalytically-active oxide radicals.

The catalytic efficiency of hydrogen, nitrogen, chlorine, and bromine oxides is determined by a set of interlocking reactions which convert the active oxides to catalytically-inactive temporary reservoirs, such as HNO_3, HCl, $ClONO_2$, H_2O, HOCl, HOBr, and $BrONO_2$, and vice versa. In the lower stratosphere, the balance between catalytic oxides and temporary reservoirs is strongly affected by reactions on the surfaces of stratospheric aerosols. The balance is even more profoundly affected in the polar winter by reactions on the surface of Polar Stratospheric Cloud (PSC) particles. In the early spring, the chlorine balance is shifted to almost 100% ClO_x (ClO_x is shorthand for the sum of all chlorine radicals, C1O, Cl_2O_2, Cl) (Brune et al. 1989; Waters et al. 1993). This shift in the chemical balance results in a large calculated chemical sensitivity of ozone towards chlorine perturbations and a relatively small calculated sensitivity of ozone towards nitrogen oxide perturbations.

Although the basic outline of the chemistry controlling stratospheric ozone is now known, many important aspects of the problem remain to be solved. The primary difference between the Northern and Southern Hemispheric polar ozone loss regions appears to be a result of the "denitrification" that occurs in the Antarctic winter. Denitrification means the removal of nitrogen oxides and HNO_3 by large particles which fall into the troposphere. Denitrification takes place when temperatures are cold enough to form large stratospheric ice crystals.

When springtime comes there are no nitrogen oxides to convert ClO_x to $ClONO_2$ and slow down the rate of ozone depletion. There is some evidence for denitrification when temperatures are not cold enough to form ice crystals. Under those conditions the mechanism for denitrification is not completely understood.

7.1.3.2 Transport

Much of the currently-observed ozone interannual variability in the stratosphere is controlled by dynamical processes. In particular, this variability is driven by such processes as the quasi-biennial oscillation (QBO), El Niño-Southern Oscillation, tropospheric weather systems which extend into the stratosphere, and long-term fluctuations in planetary wave activity. The annual cycle of total ozone is largely driven by transport effects. As shown in Figure 7.2, relatively low values of ozone are observed in the tropics and high values are observed in the extratropics. These low tropical ozone values occur in spite of the large ozone production rates in the tropics. If ozone production were precisely balanced by ozone loss everywhere, total ozone would have extremely high values in the tropics. The observed tropical low values result from vertical advection of low-ozone air from the tropical troposphere into the tropical stratosphere, and the subsequent transport of this air poleward and downward into the extratropics and polar regions. This advective circulation is known as the Brewer-Dobson circulation.

The redistribution of ozone from the production region at low latitudes to extratropical latitudes is modulated by a variety of processes. Foremost among these processes is the annual cycle in the circulation. It is now recognized that the Brewer-Dobson circulation is primarily controlled by large-scale waves in the winter stratosphere. As these waves propagate through the westerly winds that dominate the winter stratosphere, they exert a westward zonal drag, which through the Coriolis force leads to a poleward and downward transport circulation, which in turn drives the temperatures away from radiative equilibrium. The large-scale waves breaking in the winter upper stratosphere also produce lifting in the tropics. Since the lifetime of ozone increases with pressure, the poleward downward circulation causes ozone to accumulate in the lower stratosphere over the course of the winter. Since the large-scale waves are not present in the summer, the poleward and downward circulation is significantly weakened, and ozone amounts which have built up during winter begin to decrease due both to transport into the troposphere and to photochemistry.

The exchange of mass between the troposphere and the stratosphere is the focus of considerable current research (Holton et al. 1995). Stratosphere-troposphere exchange is important for the budget of ozone in the lower stratosphere as well as the ozone budget in the troposphere. Upward transport occurs in the tropics, but the exact mechanism controlling the transport is not clear. Current research is focussing on the role of subvisible cirrus and the radiative impact of infrared (IR) heating of subvisible cirrus (Jensen et al. 1997). Downward transport (stratosphere to troposphere) takes place in midlatitudes through jet stream folds—but the frequency and amount of mass irreversibly moving through these folds is still not understood (Holton et al. 1995).

7.1.3.3 Aerosols and Polar Stratospheric Clouds (PSCs)

It is now known that knowledge of stratospheric aerosols and PSCs is very important to our understanding of stratospheric ozone. The surfaces of aerosols and PSCs are sites for heterogeneous reactions which can convert chlorine from reservoir to radical forms. Likewise, radical nitro-

gen forms can be sequestered as nitric acid to shift the chemical loss process (WMO 1995).

7.1.3.3.1 Aerosols

The long-term stratospheric aerosol record reveals at least three components: episodic volcanic enhancements, PSCs and clouds just above the tropical tropopause, and a background aerosol level. At normal stratospheric temperatures, aerosols are most likely super-cooled solution droplets of H_2SO_4-H_2O, with an acid weight fraction of 55 to 80%. The primary source of stratospheric aerosols is volcanic eruptions that are strong enough to inject SO_2 buoyantly into the stratosphere. Aerosol sizes range from hundredths of a micrometer to several micrometers. Although there is some variability, especially just after a volcanic eruption, a log-normal size distribution of spherical particles appears to aptly describe the aerosol. Just after an eruption, the size distribution becomes bimodal, and some particles are nonspherical because of the addition of crustal material. After an eruption, the SO_2 is converted to H_2SO_4, which condenses to form stratospheric sulfuric acid aerosols, with a time scale of about 30 days. Subsequently, aerosol loading decreases due to a combination of sedimentation, subsidence, and exchange through tropopause folds. The loading decreases with an e-folding time of 9-to-12 months, although this appears quite variable with altitude and latitude.

The net effect of this post-volcanic dispersion and natural cleansing is a greatly enhanced aerosol concentration in the upper troposphere after a major eruption, especially poleward of about 30° latitude. Except immediately after an eruption, stratospheric aerosol droplets tend to be concentrated into 3 distinct latitudinal bands—one over the equatorial region (to 30°) and the other over each high-latitude region, 50˚ to 90° N and S. Following a low-latitude eruption, aerosol is dispersed into both hemispheres, whereas following a mid-to-high-latitude eruption, aerosols tend to stay primarily in the hemisphere of the eruption. Potential sources of a background aerosol component include carbonyl sulfide (OCS) from the oceans, low-level SO_2 emissions from volcanoes, and various anthropogenic sources, including industrial and aircraft emissions. Also, it is not clear whether there is an upward trend in this background aerosol, as has been hypothesized and linked to increasing aircraft emissions, since any increase may be due to incomplete removal of past volcanic aerosol.

Stratospheric aerosol loading in 1979 was approximately 0.5×10^{12}g (0.5 Mt), thought to be representative of background aerosol conditions. The present status of the aerosol is one of enhancement due to the June 1991 eruption of Pinatubo (15.1° N, 120.4° E), which produced on the order of 30×10^{12}g (30 Mt) of new aerosol in the stratosphere, about 3 times that of the 1982 eruption of El Chichón. This perturbation appears to be the largest of the century, perhaps the largest since the 1883 eruption of Krakatoa. By early 1993, stratospheric loading decreased to approximately 13 Mt, about equal to the peak loading values after El Chichón (McCormick et al. 1995). Measurements in 1995 showed that the aerosol levels were approaching background levels.

7.1.3.3.2 Polar Stratospheric Clouds (PSCs)

The interannual variability in PSC sightings has been addressed by Poole and Pitts (1994), who analyzed more than a decade of data from the spaceborne Stratospheric Aerosol Measurement (SAM) II sensor (Figure 7.6). They found noticeable variability in PSC sightings in the Antarctic from year to year, even though the southern polar vortex is typically quite stable and long-lived. This variability was found to occur late in the season and can be explained qualitatively by temperature differences. Poole and Pitts found even more year-to-year variability in SAM II Arctic PSC sighting probabilities. This was expected since the characteristics and longevity of the northern polar vortex vary greatly from one year to the next. The year-to-year variability in Arctic sighting probabilities can also be explained qualitatively by differences in temperature, e.g., zonal mean lower stratospheric temperatures in February 1988 were as much as 20 K colder than those one year earlier.

7.1.3.4 Solar ultraviolet and energetic particles

Since ozone formation is fundamentally linked to the levels of ultraviolet radiation reaching the Earth, natural variations in that radiation must be understood in order to detect trends. The ultraviolet comprises only one-to-two percent of the total solar radiation, but it displays considerably more variation than the longer wavelength visible radiation. For example, from 1986 to 1990 the solar UV increased with onset of the 11-year solar cycle and resulted in an increase of global total ozone of almost 2%. This natural increase in ozone is comparable to the suspected anthropogenic decrease and needs to be understood in order to totally separate the anthropogenic decrease from this natural change. Studies of total ozone trends typically subtract solar cycle and other natural changes from the total ozone record in trend resolution (see WMO 1992; WMO 1995; Stolarski et al. 1991; and Hood and McCormack 1992). Thus, more-quantitative knowledge of this natural solar-cycle-induced total ozone change would be especially valuable.

Changes in energetic particle flux from the sun penetrate into the middle atmosphere and may also drive

the natural ozone variations. A series of solar flares in 1989 spewed solar particles into the Earth's polar cap regions (greater than 60° geomagnetic latitude) and led to polar ozone depletion (Jackman et al. 1993). Further studies related to the very large solar particle events (SPEs) of October 1989 have predicted ozone depletions lasting for several months after the SPEs (Reid et al. 1991; Jackman et al. 1995). Although SPEs of this magnitude occur infrequently (only two have been observed in the past 25 years), they need to be understood more completely to be able to separate natural from anthropogenic ozone effects.

Relativistic electron precipitations (REPs) have been predicted to contribute substantially to the odd nitrogen budget of the stratosphere and, therefore, have been predicted to play a large role in controlling ozone in this region (Callis et al. 1991a, 1991b). Another investigation (Aikin 1992) has failed to find any REP-caused ozone depletion. Further work (Gaines et al. 1995) determined that REPs in May 1992, the largest measured relativistic electron flux precipitating in the atmosphere between October 1991 and July 1994, added only about 0.5 to 1% of the global annual source of odd nitrogen to the stratosphere and mesosphere. The actual importance of REPs in regulating ozone is thus not well understood nor characterized, and further work on REPs is required to thoroughly determine their importance regarding modulation of stratospheric ozone.

7.1.4 Modeling the ozone distribution, assessments

Models of the stratosphere provide the only means to attempt quantitative prediction of global change, or to evaluate the impact of natural or anthropogenic changes in composition on the stratospheric ozone and climate. In addition, models provide a means to integrate observations and theory, to provide tests of mechanisms for chemical, dynamical, or radiative changes, and to enable interpretation of observations from different platforms.

7.1.4.1 Two-dimensional models

Two-dimensional (2-D) models are used by several research groups. The models predict the behavior of ozone and other trace gases in reasonable agreement with measurements (WMO 1992; WMO 1995). Because of these favorable comparisons to measurements, these models have been utilized recently in many atmospheric studies, for example: 1) the response of the middle atmosphere due to solar variability was studied by Brasseur (1993), Huang and Brasseur (1993), and Fleming et al. (1995); 2) the influence of the Mt. Pinatubo eruption on the stratosphere was studied by Kinnison et al. (1994a, b) and Tie et al. (1994); and 3) the effects of proposed stratospheric aircraft on atmospheric constituents were studied by Pitari et al. (1993), Weisenstein et al. (1993), Considine et al. (1994), and Considine et al. (1995).

Figure 7.6

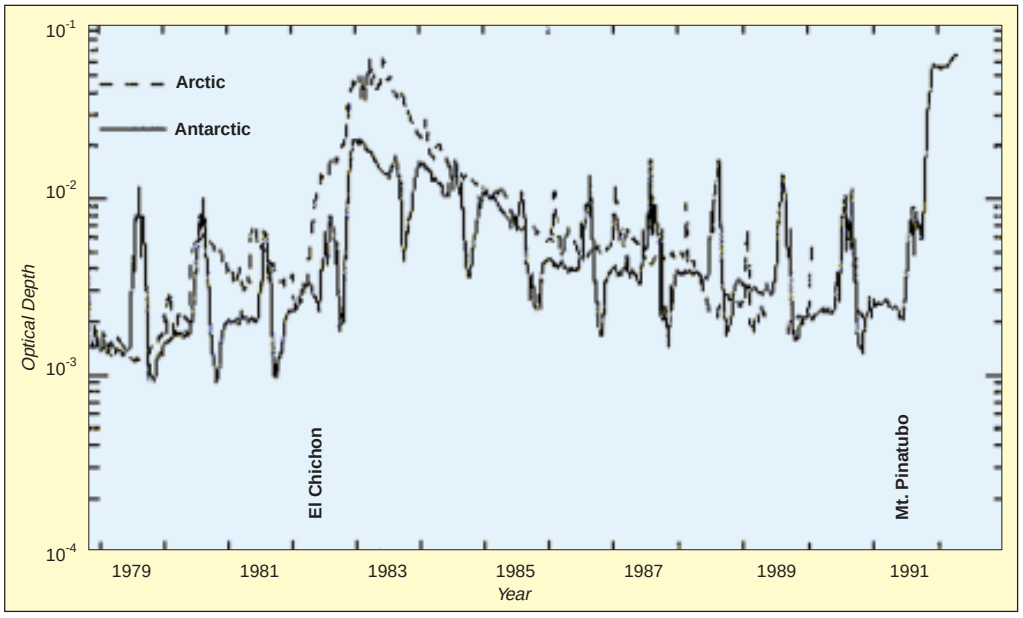

SAM II measurements of vertical optical depth data in the stratosphere over the Arctic and Antarctic. The measurements show the impact of volcanic eruptions over the period 1979-1992 along with seasonal effects in the local winters due to Polar Stratospheric Clouds (PSCs). The data are weekly averages at a wavelength of 1000 nm.

These 2-D models have also been used to produce multi-year simulations of the response of stratospheric ozone to perturbations of the source gases such as CFCs from which chlorine radicals are produced (WMO 1992; WMO 1995). An outstanding issue regarding simulations of the stratospheric ozone response to chlorine increases is the lack of ability of 2-D models to accurately predict the ozone trend in the middle and high northern latitudes over the 1980-to-1990 time period. Since the 2-D models predict a smaller trend than observed, it is believed that the models do not adequately model all of the relevant processes and thus require further development.

7.1.4.2 Three-dimensional models

The three-dimensional (3-D) (or general circulation) model with full interaction between chemical, dynamical, and radiative processes remains elusive. The present generation of general circulation models (GCMs) generates unrealistic temperature fields which, in turn, alter the photochemistry. The unrealistic temperatures are related to problems with the model transport circulation. For example, the polar regions are persistently cold in GCMs, which suggests that there is insufficient adiabatic heating (or descent) in the winter polar region. Correspondingly, there will be insufficient ascent in the tropics, which weakens the transport from the troposphere into the stratosphere.

Subtle changes in the general circulation of the atmosphere in 3-D models can alter and distort the chemical feedbacks. For example, Rasch et al. (1995) report on a two-year simulation using version 2 of the National Center for Atmospheric Research (NCAR) Middle Atmosphere Community Climate Model (MACCM2). A chemical scheme for 24 reactive species, or families, is run as part of this simulation. This model is partially coupled in that the water vapor predicted by MACCM2 is connected to the chemical source of water through oxidation of methane. Prescribed ozone is used in the radiative calculation. In this simulation, the calculated upper stratospheric ozone is substantially lower than is observed; much of the difference is attributed to the lower CH_4, compared to observations by the UARS Halogen Occultation Experiment (HALOE). This bias leads to excessive ClO and excessive destruction of O_3. In effect, the error in this long-lived trace gas, which results from the weak transport circulation, leads to noticeable errors in ozone.

The difficulties described above show why most 3-D modeling efforts have focused on "off-line" calculations, i.e., use of chemistry and transport models (CTMs) in which the wind and temperature fields are input from a GCM (e.g., Eckman et al. 1995) or from a data assimilation system (e.g., Rood et al. 1991; Lefevre et al. 1994). For either approach, there are computational advantages, as the same set of winds and temperatures is used many times. Furthermore, the effects of modifications to the chemical scheme can be isolated, and their effects understood, without the complications caused by feedback processes. A further advantage of the use of assimilated winds and temperatures is that the results of constituent simulations may be compared directly with observations with no temperature biases such as those found in GCMs. This is particularly important for the study of processes which have a temperature threshold, such as heterogeneous reactions on PSC surfaces. The most information is gleaned when the model is sampled in a manner consistent with the satellite sampling (Geller et al. 1993).

The "off-line" approach has been used successfully for many years and is used to test chemical and transport mechanisms, as well as to interpret observations. These tests include:

1) assessment of the importance of transport of air with high levels of reactive chlorine to middle latitudes (Douglass et al. 1991);

2) assessment of the rate of ozone loss within the Northern Hemisphere vortex and identification of the variables to which the calculation is sensitive (Chipperfield et al.1993);

3) determination of the importance of upper tropospheric synoptic-scale systems on the vortex temperature, as well as their influence on the transport and mixing of air which has experienced temperatures cold enough for PSC formation (Douglass et al. 1993); and

4) examination of the impact of ozone transport following the breakup of the Antarctic polar vortex on the global ozone budget (the "ozone dilution" effect).

These 3-D studies provide a picture of the important physical processes which control polar ozone loss. However, because of computer resource restrictions, it is not yet possible to make full 3-D model long-range predictions, including possible influence of the ozone loss on lower stratospheric temperature and climate. For example, future temperature changes may have a significant impact on the Northern Hemisphere vortex. The full 3-D model, with all relevant chemical, dynamical, and radiative processes and feedbacks among them, has yet to be developed.

7.2 Major scientific issues and measurement needs

Changes in the ozone layer can be divided into two categories: natural changes and man-made changes. Separating these components is the goal of much ozone and trace gas research. Since ozone can be transported by stratospheric winds, there is significant interannual variability in column ozone amounts. Ozone is likewise influenced by aerosol amounts (through heterogeneous chemistry) (Solomon et al. 1996), the formation of nitrogen radicals associated with high-energy particles, and variations in the ultraviolet radiation from the sun. Man-made changes generally include increased chlorine and hydrogen amounts from industrial gases and increased aerosols and nitrogen radicals from airplane exhaust. Many of our current scientific issues and future measurement needs center around the interaction of the ozone layer with these pollutants and separating natural changes in the ozone layer from man-made processes.

7.2.1 Natural changes

7.2.1.1 Interannual and long-term variability of the stratospheric circulation

Because the stratospheric circulation is strongly dependent on the dissipation of large-scale waves in the stratosphere, interannual variability of the wave amplitudes has an important impact on ozone transport (see Section 7.1.3.2). Winds and temperatures derived from 3-D GCMs and assimilation models include such interannual variability and can be used to assess the impact on ozone transport. 2-D models can incorporate prescribed variability to simulate interannual ozone transport (see Section 7.1.4.1). Accurate assessment of the large-scale waves and the transport circulation is necessary for understanding the variability of ozone trends.

One of the failures of the 3-D models is inadequate simulation of the QBO. The QBO is a 24-30-month oscillation of the zonal wind in the tropical lower stratosphere that is driven by tropical waves. The QBO affects the stratospheric temperature distribution and produces a secondary circulation which transports trace gases and aerosols. For ozone, the QBO can generate variations from the climatological mean of 5-10 DU in the tropics. There is also a QBO-ozone signal outside the tropics of 10-20 DU.

The QBO provides one of the largest components of the interannual variability of the column ozone values. Because the geostrophic relationship breaks down in the tropics, direct tropical wind measurements are critical to precisely measuring the QBO and for understanding the effects of the QBO on the circulation. Data-sparse regions and infrequent sampling of wind fields all preclude good quantitative studies of the tropical circulation and its effect on ozone.

7.2.1.2 External influences (solar and energetic particle effects)

As discussed in Section 7.1.3.4 solar ultraviolet radiation and precipitating energetic particles can strongly influence ozone amounts. In order to understand the anthropogenic changes in ozone, we must maintain reliable measurements of the solar ultraviolet input to the middle atmosphere. Solar variations in the UV produce ozone changes on the same order of magnitude as the current observed midlatitude changes. Proxies for the UV changes have been historically used to estimate the response of ozone to solar ultraviolet changes. With direct measurements from UARS, these proxies have been shown to inadequately represent changes in ultraviolet flux.

Particle events generate NO_x compounds which catalytically destroy ozone, but these events tend to be confined to the upper stratosphere. Large events, which tend to be more episodic, may affect polar ozone at lower levels. The impact of NO_x generation through particle precipitation on the natural ozone layer is a major scientific question.

7.2.1.3 Natural aerosols and PSCs

As discussed in Section 7.1.3.3, aerosols and PSCs are believed to play a major (although indirect) role in ozone loss. Irregular volcanic inputs of SO_2 with the subsequent formation of sulfate aerosols have an impact on the ozone layer. There is some evidence suggesting that increasing amounts of background aerosols are a result of subsonic aircraft emissions in the lower stratosphere. A major scientific question is whether the background amounts of these aerosols are increasing and, if so, determining their origin. Monitoring the aerosol amounts within the stratosphere and determining their trend is a primary measurement requirement to understand ozone loss.

During the 1980s it became apparent that aerosols play an important role in the chemistry of the stratosphere. Observations of large decreases in ozone over Antarctica during the Southern Hemisphere spring were not accounted for by theory, until several researchers hypothesized that heterogeneous reactions on PSCs might be converting inactive chlorine compounds into reactive forms (Solomon et al. 1986; McElroy et al. 1986; Toon et

al. 1986). In a similar fashion to PSCs, heterogeneous reactions upon sulfuric acid droplets at midlatitudes convert N_2O_5 into HNO_3 and shift the ratio of HNO_3 to NO_2 normally present in the stratosphere. Throughout the stratosphere, reactions on and inside aerosol particles are therefore important.

To understand the effectiveness of the heterogeneous (gas phase/aerosol phase) reactions, it is important to know:

a) the temperatures of the aerosol particles;
b) the surface and volume densities of the aerosol particles, which are derived from the aerosol extinction, and a knowledge of the size distribution;
c) the composition (the mixing ratios of H_2O, H_2SO_4, and HNO_3 in ppbv) and phase (liquid/solid/amorphous solid solution) of the aerosol particles;
d) the concentration of the reactants in the aerosol (e.g., the concentration of HCl); and
e) the duration of time over which the heterogeneous reactions occur.

A theoretical framework, by which heterogeneous rates of reaction are quantified, is given in Hanson et al. (1994).

An important research goal is the ability to observe the yearly episodes of ozone loss in the polar regions (e.g., the Antarctic ozone hole), to measure this loss as reservoir chlorine levels change with time, and to be able to relate the changes in observed ozone to a quantitative understanding of heterogeneous processes.

In principle, one should be able to identify the composition of stratospheric aerosol from multi-wavelength extinction data. Multi-wavelength observations of midlatitude sulfuric acid droplets have an extensive history. Observations of El Chichón aerosol (Pollack et al. l991), post El Chichón aerosol (Osborn et al. 1989; Oberbeck et al. 1989), and of Mt. Pinatubo aerosol (Grainger et al. 1993; Massie et al. 1994; and Rinsland et al. l994) yield spectral data consistent with theoretical expectation. Analysis of multi-wavelength observations of PSCs is a developing research topic. Recent attempts to use spectra to determine PSC composition are illustrated by Toon and Tolbert (1995).

Several years ago, ice and nitric acid trihydrate (NAT) particles were thought to be the primary composition of PSCs. Recent studies have shown that some PSC particles are liquid (the ternary solution of $HNO_3/H_2O/H_2SO_4$), and not that of crystalline NAT (Carslaw et al. l994; Drdla et al. l994). As additional laboratory cold-temperature measurements of the indices of refraction of PSC composition candidates become available, the ability to classify PSC composition from spectra will improve.

Although PSCs are now known to be instrumental in polar ozone loss, their amounts and types must be monitored. The major difference between the Antarctic ozone depletion and the less-severe Arctic depletion appears to be the result of a lack of denitrification in the Arctic (Schoeberl et al. 1993). Fundamentally, denitrification is a function of temperature and the size of PSCs. Above frost point the PSC size is generally too small to precipitate nitric acid from the stratosphere. If temperatures reach frost point, larger PSCs form, which are able to remove nitrogen acid from the lower stratosphere. The temperature history of the air parcel may play an important role in the PSC size distribution as well (e.g., Murphy and Gary 1995). Photolysis of the nitric acid is key to halting the ozone depletion during winter.

With the increase of greenhouse gases, the stratosphere is expected to cool and thus increase the probability of PSC formation as well as increase the surface area and heterogeneous reaction rates on sulfate aerosols. Preliminary studies (Austin et al. 1992) suggest greenhouse gas increase could have a major role in polar ozone depletion through increased probability of PSC formation. Monitoring stratospheric aerosol loading and PSC amounts is critical for understanding ozone loss.

7.2.2 Man-made changes

Man-made changes in ozone mostly arise from the manufacture of unreactive chlorine-containing compounds such as the CFCs (chlorine source gases). These compounds reach stratospheric altitudes where photolysis by ultraviolet radiation releases chlorine with subsequent destruction of ozone through catalytic cycles. Aviation also has an impact on ozone through the release of nitrogen radicals in aircraft exhaust. Both of these anthropogenic effects are discussed below.

7.2.2.1 Trends in chlorine source gases

As mentioned earlier, chlorine source gases and their respective trends are the major drivers behind decreases in stratospheric ozone. A comprehensive discussion of chlorine source gases is contained in WMO (1995). This report may be consulted for more detail and appropriate references.

7.2.2.1.1 Historical trends in chlorine source gases

All chlorine in the stratosphere comes from tropospheric sources, predominantly the man-made CFCs and chlorocarbons. The man-made sources account for about 7/8th of the total stratospheric chlorine. CFCs are cur-

rently being phased out in favor of the hydrochlorofluorocarbons (HCFCs). Extensive measurements of the chlorofluorocarbons CFC-11 (CCl_3F), CFC-12 (CCl_2F_2), and CFC-113 (CCl_2FCClF_2) have indicated a steady increase in their tropospheric mixing ratios for more than a decade. Most recent data suggest that the growth rate for these species has begun to decrease. Measurements taken from Tasmania suggest that levels of the important chlorocarbon CCl_4 in the troposphere are also decreasing.

As HCFCs are introduced as substitutes for CFCs, it may be expected that their mixing ratios in the troposphere will increase well into the next century. HCFC-22 ($CHClF_2$) data show a near-linear growth rate in recent years. HCFC-141b and HCFC-142b have been available only recently as CFC replacements. These species are clearly increasing in the troposphere, but further data is required to get reliable growth rates for long-term studies.

CH_3CCl_3 data also indicate a reduced growth rate that is a result of recently-reduced emissions, but also possibly due in part to increasing hydroxyl (OH) levels. Data for dichloromethane (CH_2Cl_2), methyl chloride (CH_3Cl), and chloroform ($CHCl_3$) currently exhibit no long-term trends. Continued tropospheric measurements of these gases are required to estimate ozone depletion potential.

7.2.2.1.2 Stratospheric chlorine

An extensive compilation of measurements of chlorine source gases in the stratosphere can be found in Fraser et al. (1994). The most comprehensive suites of simultaneous measurements of chlorine constituents in the stratosphere include the Atmospheric Trace Molecule Spectroscopy (ATMOS) experiments of 1985, 1992, and 1993, and the Airborne Arctic Stratospheric Expedition II (AASE II) measurements of 1991, 1992. The data from these missions have provided invaluable information on the stratospheric chlorine burden and the partitioning among the various chlorine species.

Based upon the 1985 ATMOS data, Zander et al. (1992) determined a total stratospheric chlorine level of 2.55 ± 0.28 ppbv. Further, they concluded that above 50 km most of the inorganic chlorine was in the form of hydrogen chloride (HCl), and that the partitioning of the chlorine among sources, sinks, and reservoir species was consistent with that level of total chlorine.

From the 1992 ATMOS flights, total stratospheric chlorine (based upon HCl data above 50 km) was estimated to be 3.4 ± 0.3 ppbv, an increase of approximately 35% in seven years (Gunson et al. 1994). This increase is consistent with that predicted by models (e.g., WMO 1992). Schauffler et al. (1993) inferred total chlorine levels of 3.50 ± 0.06 ppbv from the AASE II data near the tropopause, a value which is in excellent agreement with the 1992 ATMOS values.

Recent HCl data (55 km) from HALOE on UARS (see Russell et al. 1996) reveal a trend in HCl versus time at 55 km (v18) compared with the estimated total Cl trend based on tropospheric emissions (Figure 7.7).

Of the total stratospheric burden, only about 0.5 ppbv is estimated to arise from natural sources in the troposphere (WMO 1995), but these estimates have yet to be confirmed by direct or remote observations. HCl emissions from major volcanic eruptions (El Chichón, 1982, and Mt. Pinatubo, 1991) provided negligible perturbations to the levels of HCl in the stratosphere (Mankin and Coffey 1984; Wallace and Livingston 1992; and Mankin et al. 1992).

7.2.2.1.3 Depletion of ozone by stratospheric chlorine

Estimates of the severity of ozone depletion in the future can only be determined by atmospheric model simulations. The level of confidence in these models is based upon their ability to simulate present atmospheric distributions and their ability to simulate recent (decadal) trends. A discussion of the strengths and weaknesses of current assessment models is contained in WMO (1995) and Section 7.1.4.1.

Model simulations of ozone change spanning the period 1980 to 2050 were conducted as part of the WMO (1995) assessment process. Two scenarios were adopted for the assessment studies: 1) the emissions of halocarbons follow the guidelines in the Amendments to the Montreal Protocol, Scenario I; and 2) partial compliance with the guidelines, Scenario II (see WMO [1995] for specific details of the scenarios and models).

Figure 7.8 (pg. 324) summarizes the results of the model calculations for Scenario I. This figure shows the percent change (relative to 1980) in the ozone column at 50° N in March for each of the models participating in the assessment. Decreases of up to approximately 6.5% are seen to occur just prior to 2000. The recovery time to 1980 levels varies widely for the different models, from as early as 2020 to well past 2050. The individual models all showed reasonable agreement among themselves for the present-day ozone distributions, but begin to differ substantially as the atmosphere is perturbed away from its existing state by increasing levels of nitrous oxide, methane, halocarbons, and other influences.

Uncertainties in the absolute levels of depletion predicted by the models are difficult to evaluate for these long-term scenario calculations. The trends in the source gases are changing, and the trends in the stratospheric reservoir gases, which are dependent on transport into the

stratosphere, will respond. Thus, measurements of the chlorine source and stratospheric reservoir gases must be made to test models against observations. Critical gases in the suite of required measurements are the reservoirs HCl and $ClONO_2$. The predictive capability of these assessment models directly rests on additional measurements of chlorine source gases, reservoir gases, and gases which are sensitive to transport processes.

7.2.2.2 Effects of aircraft exhaust

Long-lived source gases (e.g., N_2O, CH_4) are unreactive in the troposphere and hence can enter the stratosphere at the ambient tropospheric concentrations. In the stratosphere, these gases undergo photolysis or react with radicals to release their potential ozone-destroying catalytic agents. In contrast, aircraft flying in the stratosphere will directly inject catalytic agents into the stratosphere. The primary agents for potential ozone change which have been considered in studies of aircraft exhaust are the nitrogen oxides (NO_x) and water vapor (which leads to HO_x). Now that heterogeneous reactions on background aerosols and PSCs are known to play an important role in the ozone balance of the stratosphere, the evaluation of the effects on ozone of NO_x from supersonic aircraft flying in the stratosphere has changed significantly.

The impact on column ozone of a fleet of supersonic transports (now referred to as High Speed Civil Transports [HSCTs]) is now calculated to be of the order of 1% or less. An important possibility is that the sulfur in the exhaust will lead to the generation of numerous small particles which will add to the aerosol surface area. An increase in surface area will enhance the conversion of chlorine from its reservoirs to ClO_x and thus could lead to an increased loss rate for ozone. Another possibility is that the other condensibles in the exhaust, water vapor, and nitric acid (from NO_x) could impact the formation or duration of PSCs. Initial calculations show this effect to be small (Considine et al. 1995), and transport studies show that injection into the polar vortex is unlikely (Sparling et al. 1995), but there is still uncertainty about what will happen as the stratosphere cools with increasing CO_2 concentrations.

All of the chemical effects of HSCT exhaust depend on how much of the exhaust products accumulate in the stratosphere and where they accumulate. The same is true for the exhaust of the subsonic fleet, which is released in the upper troposphere and lower stratosphere. The three major potential effects of the subsonic fleet of aircraft are ozone increase due to the smog-like photochemistry of NO_x, CO_2 increase due to fuel consumption, and cirrus cloud formation from the water vapor. The importance of aircraft NO_x to ozone generation in the upper troposphere and lower stratosphere is not completely understood. Aircraft NO_x sources have to be compared to the NO_x sources due to lightning, stratospheric intrusions, and the lofting of ground-level pollution in cumulus clouds. Thus the role of aircraft as a source of upper tropospheric NO_x and its impact on lower stratospheric ozone is uncertain. Also uncertain is whether heterogeneous chemistry on ice crystals plays a significant role in the NO_x budget.

Understanding the impact of supersonic and subsonic aircraft exhaust on the stratospheric chemical balance is a complex problem. Knowledge of meteorological conditions is required to compute exhaust dispersion. Knowledge of aerosol chemistry is required to understand the aerosol formation process (from sulfur in fuels) and its impact on the background conditions. Finally, a good understanding of the lower stratosphere chemistry is required to understand the direct impact of the NO_x pollutants.

7.2.3 Summary of science issues

The investment by the scientific community in instrument and model development has produced a significant increase in the understanding of stratospheric chemical and dynamical processes. Although some fundamental questions of ozone loss have been answered, new questions have arisen. For example, the long-term response of the ozone layer to natural fluctuations (QBO, El Niño, volcanoes) is still not well understood (Section 7.2.1.1). The secular decrease in ozone following the eruption of Mt. Pinatubo was clearly associated with aerosol loading of the stratosphere—but the nearly one-year delay in the appearance of maximum ozone loss is still not explained. More fundamentally, the midlatitude trend in column ozone loss reported by Stolarski et al. (1991) is still not explained (although it is probably connected with the increase in stratospheric chlorine and the stratospheric chemistry associated with aerosols, see Section 7.1.3.3). Our understanding of the more-subtle chemical processes is still quite incomplete, which increases our uncertainty in the forecast predictions.

Under the Atmospheric Effects of Aviation Program (AEAP) the impact of stratospheric and tropospheric aircraft pollution on stratospheric ozone is now being investigated (Section 7.2.2.2). The research studies have reemphasized that our understanding of stratospheric transport is not complete with regard to transport, especially the containment of the pollutants within the midlatitude release regions and the distribution and magnitude of stratosphere-troposphere exchange, especially exchange of ozone. Many of the issues associated with the stratospheric circulation (Section 7.2.1.1) are above the observing range of current stratospheric aircraft (i.e.,

above 70 hPa). The analysis of UARS measurements has also revealed the tremendous advantages of global chemical data sets.

Finally, the most extensive observations of solar UV and energetic particle impact on ozone have been made recently by UARS. Unfortunately, these observations have been made during the declining phase of the solar cycle, and we have not developed a long-enough baseline of measurements to quantify the impacts of changing solar conditions. Long-term measurements of solar UV and total solar irradiance are needed during the waxing phase of the solar cycle.

Figure 7.7

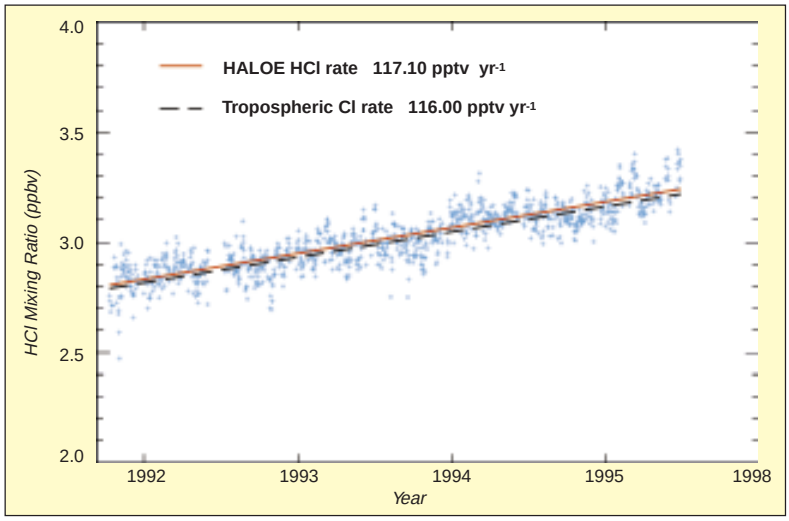

Trend in HALOE HCl versus time at 55 km (v18) compared with the estimated total Cl trend based on tropospheric emissions. Note that HCl represents ~95% of the total Cl at this altitude *(see Russell et al., 1996).*

7.3 Required measurements and data sets

The measurement requirements are discussed below. Table 7.1 (pg. 326) summarizes the minimum measurements, their accuracies, and the instruments which will make the measurements. Often, key measurements will be made by more than one instrument, which gives the whole measurement suite a level of robustness in case of instrument failure.

7.3.1 Meteorological requirements

An understanding of the photochemistry of the stratosphere is clearly contingent on high-quality observations of temperature. The temperature field affects stratospheric physical processes in a number of ways. First, temperature fields are used to calculate geopotential heights and winds via the hydrostatic and geostrophic approximations. Second, temperatures affect the radiation field, particularly in relation to the longwave cooling in the stratosphere. Third, temperatures affect the chemistry via temperature-dependent reaction rates, and via the formation of PSCs (the indirect cause of the ozone hole). Hence, accurate and precise temperatures provide a basic foundation for stratospheric chemistry, radiation, dynamics, and transport.

As stated in section 7.2.1.1 low-quality tropical meteorological observations are an impediment to our understanding of the interaction of the tropics and the middle latitudes.

The National Plan for Stratospheric Monitoring 1988-1997 (1989) set down the minimum requirements for meteorological variables between 1000 and 0.1 hPa. Their requirements were: 2.7-km vertical resolution; 12-hour time resolution; 1-K precision for temperature, and 5 m s^{-1} precision for winds.

Current radiosonde and rawinsonde measurements have precisions of a few tenths of a kelvin and 1-4 m s^{-1} wind speed in precision (Nash and Schmidlin 1987). Unfortunately, the balloon-borne rawinsonde system is limited to altitudes below 30 km. For higher altitudes, the meteorological rocket network provided some data, but the network has been effectively discontinued. Satellite systems are now relied upon to provide all of the meteorological information above 30 km.

The National Oceanographic and Atmospheric Administration (NOAA) TIROS Operational Vertical Sounder (TOVS) (Microwave Sounding Unit [MSU], Stratospheric Sounding Unit [SSU], and High-Resolution Infrared Sounder [HIRS]) SSU instrument has an error of 2 K at 10 hPa rising to 4 K at 1 hPa. The TOVS weighting functions are about 10-12-km deep. Later NOAA sounders use the Advanced Microwave Sounding Unit (AMSU) instead of MSU/SSU. The AMSU weighting functions are about half the depth of the TOVS functions. AMSU temperature measurements are limited to the atmosphere below 50 hPa.

Figure 7.8

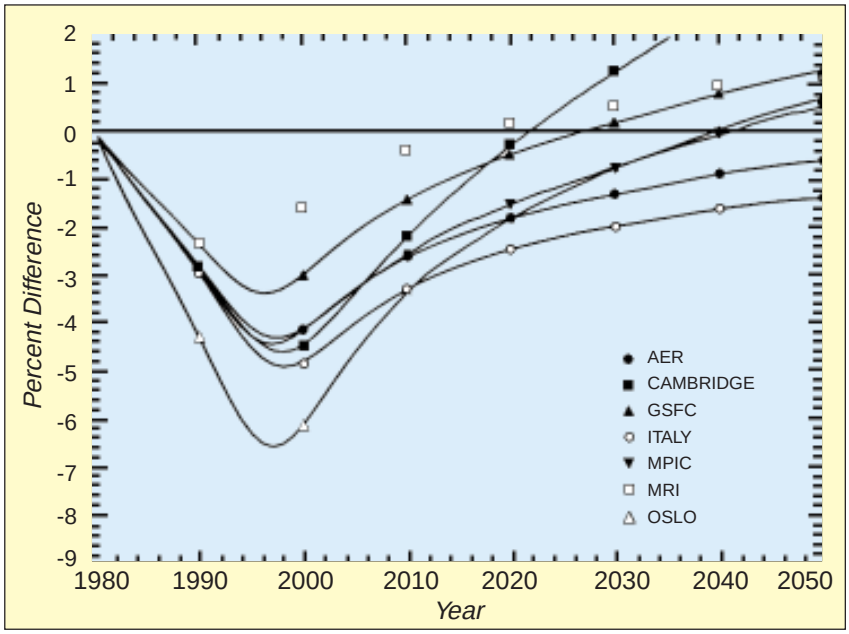

A summary of model calculations of the percent change in column ozone versus time for March at 50° N for Scenario 1 ***(reproduced from Fig. 6-12 of WMO 1995).***

The UARS Microwave Limb Sounder (MLS) has a vertical resolution of a few km, although its horizontal coverage is inferior to nadir-sounding TOVS and AMSU instruments. Improved understanding of stratospheric chemistry and heterogeneous processing suggests that improvement of temperature measurements will have an impact on our ability to predict where the heterogeneous reactions will take place.

Lower stratospheric temperature measurements made during the numerous polar aircraft missions suggest that the meteorological analyses (based upon TOVS) in the Southern Hemisphere are warm biased by about 2 K. This suggests that the Earth EOS stratospheric temperature accuracy requirements should be less than 0.5 K. It is also important that good temperature measurements be made near the tropical tropopause, especially in cloudy regions where air is entering the stratosphere through the tropopause.

Direct stratospheric wind data are needed where the divergence fields are significant (e.g., the tropics). The current wind requirement for assimilation models is an unbiased horizontal wind field accuracy of 2-5 m s^{-1}. These should be global measurements with a vertical resolution of a few kilometers. Presently, the UARS High Resolution Doppler Imager (HRDI) satellite wind instrument makes these measurements at the upper end of the limit.

A joint effort between NOAA, the Department of Defense, and NASA will produce the National Polar Orbiting Environmental Satellite System. This system will take needed operational data and certain long term observations for climate studies (Integrated Program Office, IPO, 1996, 1998). This system will be in place after 2008. The requirements for meteorological variables between 1000 and 1 mb include the following: temperatures accuracys of better than 1.5 K with vertical resolutions of 1 to 5 km from the ground to the mesosphere. The local revisit time is 6 hours and horizontal cell size of about 50 km. The NPOESS also has operational requirements for total column and profile ozone, aerosols and winds (IPO, 1996, 1998).

7.3.2 Chemical measurement requirements

Atmospheric composition measurements form a cornerstone of any global change strategy. Chemical and dynamical measurements must be made in both the stratosphere and the troposphere. Indeed, chemical measurements around the upper troposphere and lower stratosphere should be among those with the highest priority.

7.3.2.1 Science questions

The science questions for stratospheric processes are mostly focused on the changes in the stratosphere expected to take place as anthropogenic pollutants accumulate in the middle atmosphere. Greenhouse gases are expected to substantially increase during the EOS period. Stratospheric halogens are expected to increase until 1999, then level off and slowly decline as a result of international regulations. The increases in these gases should produce chemical and dynamical changes. The magnitude of the stratospheric cooling in response to increasing greenhouse gases should far exceed the tropospheric warming because there are fewer feedback mechanisms (such as clouds) which buffer the radiative interaction. Increases in chlorine and bromine will cause decreases in stratospheric ozone. The ozone decrease could be exacerbated by colder

lower stratospheric temperatures caused by increasing greenhouse gas concentrations. For example, the colder stratospheric temperatures may lead to an expansion of the extent of PSCs and, hence, polar ozone depletion.

The complex chemistry of the stratosphere can only be understood in detail by measuring a broad range of species over varying conditions with global coverage and over at least an annual cycle. The first area which merits further observational and theoretical study is polar chemistry processes. Direct, simultaneous measurements of HOCl (or a proxy such as ClO), HNO_3, and N_2O_5 are critical since these gases are believed to be involved in PSC surface chemistry. Also, polar night observations, above 20 km, of the chemically-active species, along with PSC measurements, are needed in understanding polar ozone depletion. These regions are not presently accessible with balloons and aircraft.

In order to understand the large ozone depletion at midlatitudes (see Section 7.1.2.2), simultaneous measurements of N_2O_5, HOCl, HNO_3, and HCl are needed to assess the role of heterogeneous chemistry on background aerosols. Since OH and HO_2 drive the chemistry of the lower stratosphere, global measurements of these gases are required to evaluate ozone losses, especially any zonal asymmetries. Also, lower mesosphere observations of OH and HO_2, along with O_3 and temperature, are likely to be key links in understanding the large O_3 decrease expected to occur near 40 km as chlorine levels continue to rise. It is clear that full understanding of these changes requires not just O_3 and ClO measurements, but HO_x and NO_x measurements as well. Measurements in the lower mesosphere, where the chemistry is more simple, may provide the best data set for this analysis.

7.3.2.2 Key trace gas measurements

There are several scientific requirements to address middle-atmosphere chemistry issues:

1) The self-consistency between the source gases and the resulting active reservoir gases needs to be tested for the four major families that are important to ozone chemistry. The four families and most important species measurements required are: oxygen family (O_3), hydrogen family (H_2O, CH_4, OH, HO_2, H_2O_2), nitrogen family (N_2O, NO_2, HNO_3, N_2O_5), and chlorine family ($CFCl_3$, CF_2Cl_2, HCl, ClO, $ClONO_2$). Stratospheric chlorine is predicted by atmospheric models to increase by 20% in the next five years; thus, our understanding of the production and partitioning among the individual family constituents needs to be verified.

2) The changes in the Antarctic/Arctic lower stratosphere constituents (O_3, H_2O, ClO, OClO, HCl, BrO, N_2O, NO_2, HNO_3, N_2O_5, and aerosols) during the ozone hole period in the winter and spring need to be monitored. Since significant changes have been detected during the 1980s and 1990s in the polar regions, these geographical areas require special attention and monitoring.

3) There are a few chemical process studies which require investigation as indicated below.

   a. The HO_x family (OH, HO_2, H_2O_2) is fundamentally important in stratospheric chemistry, but the database for that group remains one of the poorest in the atmosphere. Global measurements of the latitudinal, seasonal, and diurnal variation in the HO_x family and related species, H_2O and O_3, are needed to address this deficiency.

   b. Models for the past decade have predicted less ozone in the upper stratosphere than is measured. Several species (O_3, O, NO_2, OH, and ClO) need to be measured in the upper stratosphere to help resolve this difficulty (see Section 7.1.4.1).

   c. Models, in general, predict less odd nitrogen in the lower stratosphere than observed. Measurements of odd nitrogen species, NO_2, HNO_3, N_2O_5, and $ClONO_2$ in the lower stratosphere will help to deal with this problem.

   d. Another odd nitrogen species, HNO_3, is not modeled accurately in the wintertime in the mid-to-high latitudes. A measurement of HNO_3, N_2O_5, H_2O, and aerosols should help confront this problem.

4) Global observations of ozone in the lowermost stratosphere (tropopause to about 20 km) with high horizontal, vertical, and temporal resolution are needed in order to quantify the ozone budget in that region of the atmosphere and, in particular, to determine the spatial and temporal distribution of ozone fluxes from the lowermost stratosphere to the troposphere. These fluxes, which are presently known only to within about a factor of two, are important for the ozone budget of the lowermost stratosphere and are crucial for understanding the ozone budget of the upper troposphere.

The measurement requirements to attack these science questions are outlined in Table 7.1. Generally, the

Table 7.1

Measurement	Accuracy	EOS Instrument
Meteorology		
Temperature	1K	MLS, HIRDLS, SAGE III
Winds	2-5 m/s	(none)
Chemistry		
O_3 (column)	15 milli-atm-cm	TOMS, OMI
O_3 (profile)	0.2 ppm	MLS, HIRDLS, SAGE III
H_2O	0.5 ppm	MLS, HIRDLS, SAGE III
CFC-11 / 12	0.2 ppb	HIRDLS
N_2O	20 ppb	MLS, HIRDLS
CH_4	0.1 ppm	HIRDLS
HCl	0.1 ppb	MLS
$C1ONO_2$	0.1 ppb	HIRDLS
HNO_3	1.0 ppb	HIRDLS, MLS
NO_2 / NO	0.2 ppb	HIRDLS, SAGE III
C1O	50 ppt	MLS
BrO	5 ppt	MLS
OH	0.5 ppt	MLS
N_2O_5	0.2 ppb	HIRDLS
Aerosols	Surface area within 10%	SAGE III, HIRDLS
Solar Flux	100-400 nm to 4%	SOLSTICE

Stratospheric chemical and dynamical measurement requirements. Requirements include vertical resolution of 1-2 km through the tropopause into the lower stratosphere. Horizontal resolution is minimally that of UARS (2700 km), but increased horizontal resolution vastly improves the science. HIRDLS scanning will achieve a horizontal resolution of 400 km. AMLS may achieve a horizontal resolution of 100 km with MMIC array technology.

accuracies needed are 5-10% of the ambient concentrations found in the lower stratosphere.

7.3.3 Stratospheric aerosols and PSCs

The remote sensing of the composition of aerosol at midlatitudes is fairly straightforward. However, remote sensing of the composition and phase of the aerosol particles, for the case of the PSCs, is a developing topic of research. One research goal is to see to what extent it is possible to estimate the composition, phase, area, and volume densities from orbital observations. It is known that the volume densities of NAT and ternary particles are different. Carslaw et al. (l994) and Drdla et al. (1994) have shown that ternary solutions best describe some of the NASA High-Altitude Research Aircraft (ER-2) data. For example, Figure 7.9 shows a graph of temperature versus volume density for several aerosol compositions. Beginning with a sulfuric acid droplet core, the volume density of the aerosol increases as temperatures become colder. These equilibrium curves were calculated using different amounts of ambient HNO_3 (5, 10, and 15 ppbv). Remote-sensing observations of temperature versus volume density (and/or aerosol extinction) will likely help classify the composition and phase of the PSC particles. It is also known that HNO_3 is incorporated in ternary, nitric acid dihydrate (NAD), and NAT particles as a function of temperature (i.e., curves of temperature versus the equilibrium gas phase of HNO_3 differ for the three compounds). Therefore, the simultaneous observation of aerosol extinction and HNO_3 gas mixing ratios should

help one to classify regions of PSCs as to composition and phase.

Since the microphysics of PSC particles is very temperature sensitive, absolute temperatures need to be measured to plus-or-minus 2 K, since curves of temperature versus volume density for NAT, ternary, and NAD particles (Figure 7.9, pg. 329) differ by only a few kelvins. Remote-sensing observations also average over many kilometers along a horizontal ray path. Vertical coverage is usually on the order of several km. Thus, the fine-scale structure of PSCs, as sampled by ER-2 instruments, cannot be resolved by the remote sounder. Another complication is due to present limitations in the theoretical understanding of how PSCs form, which compositions are formed, and the need for additional laboratory work to quantify at cold stratospheric temperatures the rates at which realistic PSC particles convert inactive to active chlorine compounds, and the need for additional laboratory measurements of the refractive indices of PSC and sulfuric droplets. Current research will see to what extent it is possible to refine present capability to quantify the mechanisms of PSC chemistry, as observed from orbit.

7.3.4 Solar ultraviolet flux

Solar radiation at wavelengths below about 300 nm is completely absorbed by the Earth's atmosphere and becomes the dominant direct energy input, establishing the composition and temperature through photodissociation, and driving much of the dynamics as well. Even small changes in this ultraviolet irradiance will have important and demonstrable effects on atmospheric ozone. Radiation between roughly 200 and 300 nm is absorbed by ozone and becomes the major loss mechanism for ozone in the middle atmosphere. Likewise, solar radiation < 200 nm is absorbed predominantly by molecular oxygen and becomes a dominant source of ozone in the middle atmosphere, so changes in these ultraviolet wavelengths will have, to first order, an inverse influence on ozone. These two atmospheric processes, driven by solar radiation, become the major natural control for ozone in the Earth's stratosphere and lower thermosphere. To fully understand the ozone distribution will require many coordinated observations and, in particular, a precise measurement of the solar ultraviolet flux.

The visible portion of solar radiation originates in the solar photosphere and has been accurately measured for about fifteen years (Willson and Hudson 1991). Apparently, this radiation varies by only small fractions of one percent over the 11-year activity cycle of the sun, with comparable variation over time scales of a few days. The ultraviolet portion of the solar spectrum comprises only about 1% (approximately 10 W m^{-2}) and originates from higher layers of the photosphere. As we move to shorter and shorter wavelengths, the emission comes from higher and higher layers of the solar atmosphere. Unlike the solar photosphere, these higher levels are much more under the influence of solar activity, as manifested, for example, by increasing magnetic field strength. As the magnetic activity increases or disappears, the solar radiation, especially the ultraviolet, undergoes dramatic variations modulated by the 27-day rotation period of the sun. Near 120 nm the variation over time periods of days to weeks can be as large as 50%, and over the longer 11-year solar cycle the variation can be as large as a factor of two (Rottman 1993). Toward longer wavelengths, the solar variability decreases to levels of about 10% at 200 nm (Figure 7.10) and finally to only about 1% at 300 nm. Longward of 300 nm, the intrinsic solar variability is probably only on the order 0.1%, roughly commensurate with measurements of total solar radiation.

The challenge during the EOS time period is to provide measurements of the solar ultraviolet with a precision and accuracy capable of tracking the changes in the solar output. Ideally, the instrument will be capable of measuring changes as small as one percent throughout the EOS mission. This requirement is extremely challenging for solar instruments, especially those making observations at the ultraviolet wavelengths, which are notoriously variable. The harsh environment of space, coupled with the energetic solar radiation, rapidly degrades optical surfaces and usually makes the observations suspect. Some manner of in-flight calibration is required to unambiguously separate changes in the instrument response from true solar changes.

7.3.5 Validation of satellite measurements

The role of validation of satellite-based chemical measurements cannot be over stressed. Validation measurements, especially measurements of the same species using two different techniques, have proved to be invaluable for understanding satellite trace species measurements. The very successful UARS validation campaign has contributed a great deal to understanding the individual UARS measurements. The validation campaigns perform two major functions. First, they test the ability of a satellite instrument to make a measurement by giving an independent data point to compare against. Second, if the validation measurements are performed as part of a larger, coordinated campaign, the validation measurements done using aircraft and ground-based measurements can be used to link the small-scale geophysical features that they can observe with the large-scale geophysical features observable from space.

7.4 EOS contributions

7.4.1 Improvements in meteorological measurements

7.4.1.1 Global limb temperature measurements

The tropopause, the boundary between the upper troposphere (UT) and lower stratosphere (LS), is critical for understanding many important processes in the atmosphere. The tropopause is defined by a sharp change in the vertical temperature gradient, taking place over a few hundred meters at most. Below the tropopause, the troposphere is a region of active vertical mixing. Above the tropopause, the stratosphere is very stable with little vertical mixing. The match between these dissimilar regions, troposphere and stratosphere, modulates the processes that permit the exchange of mass, trace gases, momentum, potential vorticity, and energy between the two regions.

Unfortunately, present observing systems do not observe the UT-LS region with sufficient detail. The NOAA operational temperature sensors are characterized by vertical resolution of the retrievals of the order of 10-12 km. The detailed structure of the tropopause is much too thin to be seen by operational systems. However, their cross-track scanning capability gives them the ability to observe horizontal scales of about 100 km (Figure 7.11, pg. 381).

Temperature profiles with much higher vertical resolution can be obtained by observing the atmospheric limb, or horizon. The improvement results from the geometry, since most of the ray path through the atmosphere is within 1-2 km of the lowest, or tangent, point. In addition, the atmospheric signal is seen against the cold background of space. These factors can reduce the height of the vertical weighting functions to 3-4 km, and the effective resolution to ~ 5 km.

EOS limb sounders (MLS and the High-Resolution Dynamics Limb Sounder [HIRDLS] on the EOS Chemistry Mission [CHEM]) will greatly improve the accuracy, precision, and resolution of temperature measurements in the tropopause region. HIRDLS will determine temperatures with a resolution of 1-1.5 km, through a combination of a narrow (1 km) vertical field of view (FOV), low noise, and oversampling. MLS will make limb temperature measurements with a resolution of 2-3 km.

7.4.1.2 Higher horizontal resolution temperature profiles

Previous limb scanners have retrieved temperatures with higher vertical resolution, but, because the vertical scans are made at a single azimuth relative to the orbital plane, the horizontal resolution was limited to the orbital spacing, or about 25°. This is sufficient to resolve only about 6 longitudinal waves. However, the UT-LS is a region in which smaller-scale waves from the troposphere are present. The horizontal resolution of previous limb sounders did not allow these smaller-scale systems to be measured. Figure 7.11 shows that the consistent scaling between vertical and horizontal scales suggests that higher horizontal resolution is required to sample geostrophic motions. The figure shows that HIRDLS has the ability to observe and retrieve with a 1-km vertical resolution and 4° horizontal resolution by scanning from side to side. This resolution allows all horizontal waves, up to ~ wavenumber 45, to be observed with the appropriate vertical resolution. Furthermore, the high vertical resolution of HIRDLS together with the high horizontal resolution and daily observations will for the first time provide accurate global mapping of the distribution of ozone in the lowermost stratosphere, a measurement that is crucial for determining the distribution of the flux of ozone to the troposphere, which in turn is crucial for understanding the budget of tropospheric ozone.

Recently a technological innovation has been proposed for the MLS instrument. Instead of a single heterodyne receiver, Microwave Monolithic Integrated Circuit (MMIC) arrays have been proposed at two frequencies. The array system (Array MLS [AMLS]) would allow 100-km × 100-km horizontal resolution temperature, ozone, N_2O, and water with lower power and weight. This proposed system is currently being studied by NASA.

7.4.2 Improvements in chemical measurements in the stratosphere

EOS instruments will give significantly improved stratospheric chemical measurements by having better measurement precision, particularly in the lower stratosphere, and a more-complete suite of collocated measurements, especially chemical radicals. The accuracy of the proposed instruments is close to that set down in Table 7.1. The major improvements in these chemical measurements are from MLS and HIRDLS. These two instruments (especially AMLS) are very synergistic in that HIRDLS will have high resolution in longitude as well as latitude (discussed in the previous section) while MLS will be able to make measurements in high-aerosol or cloudy regions. In addition, high-latitude coverage will be obtained on each orbit from both HIRDLS and MLS, a significant improvement from UARS, which had monthly gaps in high-latitude coverage and did not sample important periods.

The high-vertical and horizontal-resolution coverage in the upper troposphere and lower stratosphere by HIRDLS (and AMLS) is extremely important because atmospheric waves with smaller horizontal scales can penetrate to these altitudes, creating variations on small scales that are critical to our understanding of wave breaking, mixing, stratosphere-troposphere exchange of mass constituents, and perhaps chemical processing.

Figure 7.9

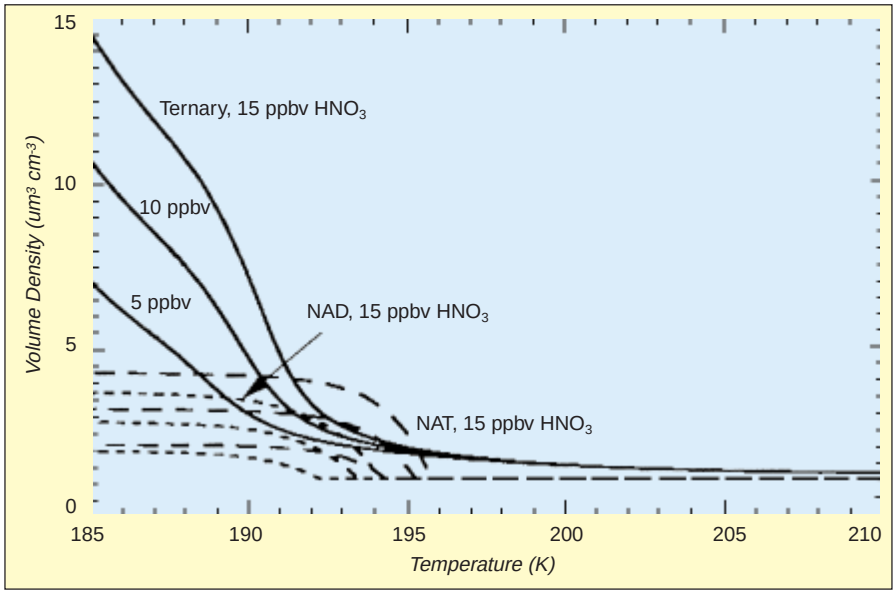

Temperature versus volume density for several aerosol compositions expected in the stratosphere.

Compared with UARS, EOS MLS has tremendous improvements in precision of lower stratospheric measurements due to its increased spectral bandwidth and choice of stronger spectral lines. Whereas UARS MLS was designed primarily for the middle and upper stratosphere, EOS MLS emphasizes the lower stratosphere. Improvements over UARS are summarized in Table 7.2.

Inclusion of the OH measurement in MLS is a major qualitative improvement in the suite of global stratospheric measurements which EOS will provide. This measurement is possible because of recent submillimeter-wavelength technology advances, which were not available for UARS. The OH measurement will extend to the lowest and the highest regions of the stratosphere, where HO_x chemistry is thought to be the dominant ozone loss mechanism on a global scale. It will cover regions where OH is thought to control the conversion of CH_4 to H_2O, to control the rates of SO_2 and OCS oxidation to sulfate aerosol, and to be an essential player in controlling the balance between radical and reservoir species in the nitrogen and chlorine families. The global OH measurements over the complete stratosphere by EOS will give unprecedented new information on stratospheric chemistry, and are especially valuable in being made simultaneously with that of the many other EOS chemistry measurements. MLS will also likely be able to measure HO_2 in the upper stratosphere, further testing and improving our understanding of stratospheric hydrogen chemistry.

HIRDLS NO_2 measurements provide an important component of NO_x, and, because of its reactions with ClO (measured by MLS), the formation of $ClONO_2$, also measured by HIRDLS. HIRDLS measurements of N_2O_5 and HNO_3, along with the $ClONO_2$, provide a fairly complete set of measurements of the NO_y (NO_y is chemical shorthand for the sum of all nitrogen reservoir and radical species, NO_x plus HNO_3, mostly) species. Note that the ratio of NO_2/HNO_3 provides an additional way of deriving the OH concentration.

MLS will also measure middle- and upper-stratospheric BrO, the dominant radical in the bromine chemical family. No global stratospheric bromine measurements have been made to date, and the BrO measurement will be important to test our understanding of this chemistry.

Other important improvements in the suite of chemical measurements include the simultaneous and commonly-calibrated measurement of HCl and ClO by MLS. This allows very accurate monitoring of the ClO/HCl ratio, which provides a sensitive indicator of our understanding of chlorine chemistry and early detection of changes. The MLS and HIRDLS N_2O measurements will allow much more accurate distinction between chemical and dynamical changes in the atmosphere.

Total ozone measurements using TOMS will continue with a flight on a Russian Meteor satellite in 2000. Total ozone measurements will continue with an advanced Ozone Monitoring Instrument (OMI) contributed to EOS Chem by the Netherlands. OMI is a hyperspectral imaging spectrometer operating in the ultraviolet and visible. Its hyperspectral capabilities will improve the precision

and accuracy of the total ozone measurements by better estimates of cloud heights and aerosols effects. OMI will make additional measurements which will be highly complimentary to EOS Chem and SAGE, such as column amounts of NO_2, background SO_2, OCLO, BrO, aerosols, and derived UV-B. After EOS-Chem, total and profile ozone will monitored by the NPOESS using an advanced TOMS and a separate profiling instrument capable of high vertical resolution measurements in the lower stratosphere.

7.4.3 Improvements in measurements of aerosols

EOS instruments will improve upon the ability demonstrated by UARS for several reasons. Temperature retrievals will be more refined, and the horizontal and vertical resolution will be better. HIRDLS resolution will be on the order of 1 km in the vertical coordinate, and 4° latitude-by-4° longitude in the horizontal coordinate, and will retrieve temperatures with an accuracy of 1K at altitudes below 50 km (Gille and Barnett 1992). The HIRDLS experiment has four spectral channels which are specifically dedicated to obtaining aerosol extinction measurements, but will obtain aerosol information from many of the other channels as well. The measurements will observe and distinguish midlatitude sulfuric acid droplets and PSCs. H_2O and HNO_3, two gases which are incorporated into stratospheric aerosols, will be retrieved by HIRDLS. In addition, $ClONO_2$ and N_2O_5, species important in heterogeneous processing, are retrieved by HIRDLS.

The SAGE III aerosol data will consist of vertical profiles of aerosol extinction at seven wavelengths extending in altitude range from the lower troposphere or cloud top to about 40-km altitude, with vertical resolution of 1 km. From the seven-wavelength aerosol extinction measurements, parameters describing the aerosol physical size distribution, such as volume density and surface area density, can be estimated with good accuracy, with uncertainties of the order of 10%. The wide spectral extinction behavior from the SAGE III measurements should also provide sufficient information to distinguish between a single-modal versus a bimodal aerosol size distribution, especially important immediately after volcanic eruptions. The SAGE III instrument will provide better tropospheric aerosol measurements with extinction measurements with multiple wavelengths through the mid-troposphere, and at least at two wave-

Figure 7.10

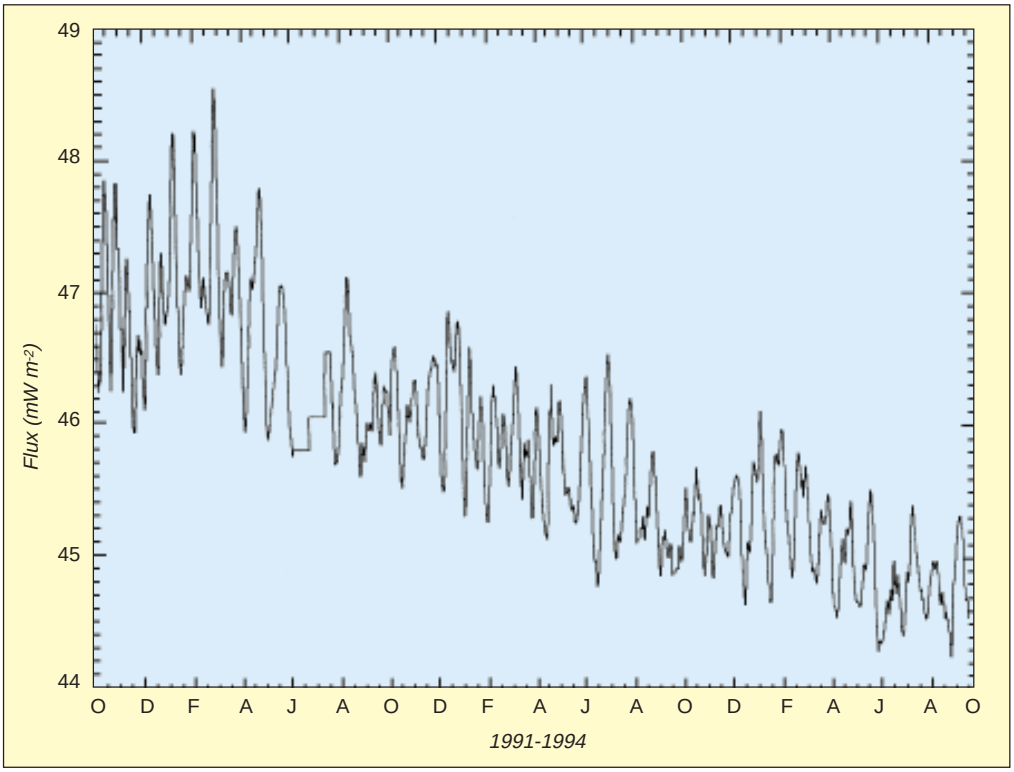

Changes in solar ultraviolet flux (200-205 nm) versus time from the UARS SOLSTICE instrument ***(Rottman et al. 1993).***

FIGURE 7.11

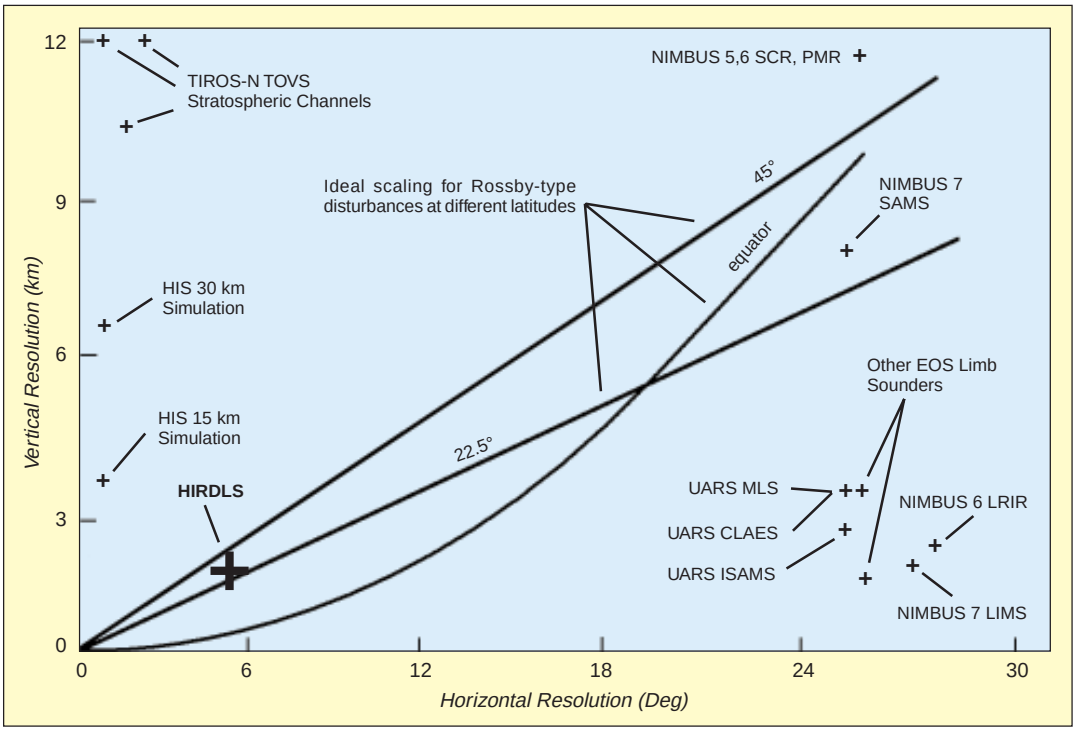

A comparison of the vertical and horizontal resolutions of various limb- and nadir-sounding satellite instruments. Lines indicate the ideal observation scale for Rossby waves.

lengths down to sea level. For the measurements of PSCs, SAGE III will be the first satellite instrument to provide size distribution information.

The SAGE III aerosol information will be key to understanding the role played by stratospheric aerosols and PSCs in heterogeneous chemical reactions and ozone depletion and will be indispensable for understanding aerosol radiative forcing.

7.4.4 Improvements in measurements of the solar ultraviolet flux

The EOS Solar Stellar Irradiance Comparison Experiment (SOLSTICE) has the unique capability of observing bright, blue stars employing the very same optics and detectors used for the solar observations. With the assumption that these stars are extremely stable, the response of SOLSTICE could be accurately monitored by observing a single star. However the calibration plan uses twenty or more of these reference stars, and it is the average flux from the entire ensemble of stars that provides an even more reliable reference for the solar observations. Repeated observation of the stars should yield an average flux level that is unchanging in time. A decrease in the level is an indication of loss in instrument sensitivity and adjustments are made accordingly. Since the same optics and detectors are used for the solar observations, the same corrections apply, and the resulting solar measurement is reliable and free of any instrumental effects. The large dynamic range between the stellar and solar signals is on the order of eight to nine orders of magnitude, and is easily accommodated by changing the entrance apertures, spectral bandpass, and integration times (Rottman et al. 1993).

7.4.5 Advanced chemical/dynamical/radiative models

EOS is currently funding a U.S. effort and cooperates with a foreign effort to build fully interactive chemical/dynamical models for interpretation of EOS data. The first effort, the Schoeberl Interdisciplinary Science Investigation (IDS), currently uses data assimilation winds and temperatures (see Section 7.4.6) along with a chemical transport model to simulate the stratospheric system. The results of this model are then used to compare with observations such as those from UARS, SAGE, and TOMS. Full coupling and feedback between the meteorology and

Table 7.2

Measurement	Instrument	Major Improvements Over UARS
O_3 (profile)	HIRDLS, MLS, OMI, SAGE III	Much better spatial resolution, much better precision (especially in lower stratosphere), continuous coverage of both hemispheres, column measurement obtained simultaneously with profile, 5× improvement in precision in lower stratosphere over UARS MLS
OH	MLS	Not measured on UARS
H_2O	HIRDLS, MLS, SAGE III	Much better spatial resolution, much better sensitivity in the tropopause region, continuous coverage of both hemispheres. 2× improvement in precision
CH_4	HIRDLS	Much better spatial resolution, much better precision, continuous coverage of both hemispheres
ClO	MLS	Much better sensitivity, continuous coverage of both hemispheres with 5× improvement in precision over UARS
BrO	MLS	Not measured on UARS
OClO	SAGE III	Not measured on UARS
HCl	MLS	Continuous coverage of both hemispheres, measurement not degraded by aerosols
$ClONO_2$	HIRDLS	Much better spatial resolution and precision, continuous coverage of both hemispheres
$CFCl_3$	HIRDLS	Much better precision than on UARS
Temperature	MLS, HIRDLS, SAGE III	10× improvement in precision over UARS
CF_2Cl_2	HIRDLS	Much better spatial resolution and precision, continuous coverage of both hemispheres
NO_2	HIRDLS, SAGE III	Much better spatial resolution, improved precision, continuous coverage of both hemispheres
NO_3	SAGE III	Not measured on UARS
HNO_3	HIRDLS, MLS	Much better spatial resolution and precision, measurements in presence of aerosols, cirrus, and PSCs, continuous coverage of both hemispheres, 20× improvement in precision over UARS
N_2O_5	HIRDLS	Much better spatial resolution, coverage and precision, continuous coverage of both hemispheres
N_2O	HIRDLS, MLS	Much better spatial resolution and precision, measurements in presence of aerosols and cirrus, continuous coverage of both hemispheres
SO_2	MLS	Continuous coverage of both hemispheres
CO	MLS	Much better sensitivity and continuous coverage of both hemispheres
HO_2	MLS	Not measured on UARS
HOCl	MLS	Not measured on UARS

Improvements in EOS Chemistry measurements over UARS.

chemistry do not occur at this stage. Later, the chemical/transport model will be used along with the EOS chemical data to produce an assimilated chemical data set. The full coupling will occur through the assimilation system. The observations of motion of long-lived trace species can be inverted to make better estimates of stratospheric winds. The forecast of temperatures from the assimilation modeling effort will increase the accuracy of the retrieved trace gases.

The second effort, the Pyle IDS (United Kingdom), uses a full GCM and chemical package. The GCM and chemical/radiation/transport system will be fully linked. The objectives are to examine the sensitivity of the atmosphere to the chemical/radiative/dynamical feedback systems. This foreign effort consists of a full-fledged EOS IDS team but is not funded by NASA.

7.4.6 Full meteorological and chemical assimilation of EOS data sets

The Data Assimilation Office (DAO) at NASA/Goddard Space Flight Center (GSFC) already provides routine support to the stratospheric aircraft missions planned to study stratospheric ozone. Daily analyses are produced for the Stratospheric Tracers of Atmospheric Transport (STRAT) mission, and, given the duration of this mission, this will evolve into the operational support of the EOS Morning Platform (AM-1). During the aircraft deployment periods, forecasts are produced to aid in-flight planning. These forecasts enhance the ability of the mission planners to target air of specific chemical characteristics.

The current DAO meteorological analyses have a large impact on stratospheric chemistry studies. The wind fields are of sufficient quality to remove the dynamical uncertainty from trace observations. This allows a high-caliber examination of chemical processes, a benefit that has been realized for satellite, balloon, and aircraft data. There are active efforts of the DAO to improve the subtropical winds and the deep vertical motions that link the stratosphere and mesosphere.

Future plans call for a straightforward extension of the application of winds from the DAO assimilation to more-general problems. This includes stratospheric-tropospheric exchange, as well as broader issues of tropospheric chemistry. Advanced assimilation systems will directly assimilate constituent observations. First, long-lived tracers will be assimilated. Initial studies of N_2O from UARS show that assimilation can in fact provide verifiable global information from the non-global UARS coverage pattern. An important goal of the DAO constituent effort is to improve wind estimates, especially in the tropics. Wind inversion techniques are being actively investigated. In addition, at least two university proposals have been recently submitted to attempt to assimilate aerosol observations within the DAO system. These proposals are examples of the long-term efforts to assimilate the complete chemical suite of measurements, with the goal of bringing to bear the quantitative analysis of data assimilation on the internal consistency of the chemical observations of UARS and CHEM.

7.5 Foreign partners and other measurement sources

Foreign partners are critical to the scientific success of the global stratospheric measurements program. The scale of collaboration ranges from individual science teams, to collaborative instruments, to reciprocal flights of instruments, to mission planning. The timing of the EOS CHEM mission has been structured to follow the launch of the European Space Agency's (ESA's) Environmental Satellite I (ENVISAT I). This mission, to be launched in 2000, follows the successful NASA UARS mission. ENVISAT will make many critical trace species measurements in the time period of maximum stratospheric chlorine. This long-term data set, UARS-ENVISAT-CHEM, will be absolutely critical to our understanding of the role of trace species in controlling ozone in the stratosphere.

Other international space platforms will carry a few stratospheric instruments: The French Systeme pour l'Observation de la Terre (SPOT) satellite will carry the Polar Ozone Aerosol Measurements II (POAM II) aerosol and ozone measuring system. The Russian MIR space station will fly the Fourier Transform Spectrometer, DOPI.

In addition to these space instruments, several stratospheric aircraft campaigns are planned for the next few years (e.g., the STRAT campaign).

References

Aikin, A. C., 1992: Stratospheric evidence of relativistic electron precipitation. *Planet. Space Sci.,* **40**, 413–431.

Anderson, J.G., D.W. Toohey, and W.H. Brune, 1991: Free radicals within the Antarctic vortex: The role of CFC's in the Antarctic ozone loss. *Science*, **251**, 39-46.

Austin, J., R. R. Garcia, J. M. Russell III, S. Solomon, and A. F. Tuck, 1986: On the atmospheric photochemistry of nitric acid. *J. Geophys. Res.*, **91**, 5477–5485.

Austin, J., N. Butchart, and K. P. Shine, 1992: Possibility of an Arctic ozone hole in a doubled-CO_2 climate. *Nature*, **360**, 221–225.

Brasseur, G., 1993: The response of the middle atmosphere to long-term and short-term solar variability: A two-dimensional model. *J. Geophys. Res.*, **98**, 23,079–23,090.

Brune, W. H., J. G. Anderson, and K. R. Chan, 1989: In situ observations ClO in the Antarctic: ER-2 aircraft results from 54 S to 72 S latitude. *J. Geophys. Res.*, **94**, 16649-16663.

Callis, L. B., D. N. Baker, J. B. Blake, J. D. Lambeth, R. E. Boughner, M. Natarajan, R. W. Klebesadel, and D. J. Gorney, 1991a: Precipitating relativistic electrons: Their long-term effect on stratospheric odd nitrogen levels. *J. Geophys. Res.*, **96**, 2939–2976.

Callis, L. B., R. E. Boughner, M. Natarajan, J. D. Lambeth, D. N. Baker, and J. B. Blake, 1991b: Ozone depletion in the high latitude lower stratosphere: 1979-1990. *J. Geophys. Res.*, **96**, 2921–2937.

Carslaw, K. S., B. P. Luo, S. L. Clegg, Th. Peter, P. Brimblecombe, and P. J. Crutzen, 1994: Stratospheric aerosol growth and HNO_3 gas depletion from coupled HNO_3 and water uptake by liquid particles. *Geophys. Res. Lett.*, **21**, 2479–2482.

Chipperfield, M. P., D. Cariolle, P. Simon, R. Ramaroson, and D. J. Lary, 1993: A three-dimensional modeling study of trace species in the Arctic lower stratosphere during winter 1989-1990. *J. Geophys. Res.*, **98**, 7199–7218.

Considine, D. B., A. R. Douglass, and C. H. Jackman, 1994: Effects of a PSC parameterization on ozone depletion due to stratospheric aircraft in a 2-D model. *J. Geophys. Res.*, **99**, 18,879–18,894.

Considine, D. B., A. R. Douglass, and C. H. Jackman, 1995: Sensitivity of two-dimensional model predictions of ozone response to stratospheric aircraft: An update. *J. Geophys. Res.*, **100**, 3075–3090.

Dobson, G. M. B., 1966: Annual variation of ozone in Antarctica. *Quart. J. Roy. Met. Soc.*, **92**, 546–550.

Douglass, A. R., R. B. Rood, J. A. Kaye, R. S. Stolarski, D. J. Allen, and E. M. Larson, 1991: The influence of polar heterogeneous processes on reactive chlorine at middle latitudes: Three-dimensional model implications. *Geophys. Res. Lett.*, **18**, 25–28.

Douglass, A. R., R. B. Rood, J. W. Waters, L. Froidevaux, W. Read, L. Elson, M. Geller, Y. Chi, M. Cerniglia, S. Steenrod, 1993: A 3-D simulation of the early winter distribution of reactive chlorine in the north polar vortex. *Geophys. Res. Lett.*, **20**, 1271–1274.

Drdla, K., A. Tabazadeh, R. P. Turco, M. Z. Jacobson, J. E. Dye, C. Twohy, and D. Baumgardner, 1994: Analysis of the physical state of one Arctic polar stratospheric cloud based on observations. *Geophys. Res. Lett.*, **21**, 2475–2478.

Eckman, R. S., W. L. Grose, R. E. Turner, W. T. Blackshear, J. M. Russell III, L. Froidevaux, J. W. Waters, J. B. Kumer, and A. E. Roche, 1995: Stratospheric trace constituents simulated by a three-dimensional general circulation model: comparison with UARS data. *J. Geophys. Res.*, **100**, 13,951–13,966.

Farman, J. C., B. B. Bardiner, and J. D. Shanklin, 1985: Large losses of total ozone in Antarctica reveal seasonal ClO_x/NO_x interaction. *Nature*, **315**, 207–210.

Fioletov, V.E. J.B. Kerr, D.I. Wardle, J. Davies, E.W. Hare, C.T. McElroy, and D.W. Tarasick, 1997: Long term decline over the Canadian arctic to early 1997 from ground based and balloon observations. *Geophys. Res. Lett.*, **24**, 2705-2708.

Fleming, E. L., S. Chandra, C. H. Jackman, D. B. Considine, and A. R. Douglass, 1995: The middle atmospheric response to short- and long-term solar UV variations: Analysis of observations and 2-D model results. J. Atmos. Terr. Phys., 57, 333–365.

Fraser, P., S. Penkett, M. Gunson, R. Weiss, and F. S. Rowland, 1994: Measurements, Chapter 1 in "NASA Report on Concentrations, Lifetimes, and Trends of CFC's, Halons, and Related Species," edited by J. Kaye, S. Penkett, and F. Ormond, NASA Reference Publication 1339, Washington, D. C., 1.1–1.68.

Gaines, E. E., D. L. Chenette, W. L. Imhof, C. H. Jackman, and J. D. Winningham, 1995: Relativistic electron fluxes in May 1992 and their effect on the middle atmosphere. *J. Geophys. Res.*, **100**, 1027–1033.

Geller, M. A., Y. Chi, R. B. Rood, A. R. Douglass, J. A. Kaye, and D. J. Allen, 1993: Satellite observation and mapping of wintertime ozone variability in the lower stratosphere. *J. Atmos. and Terr. Phys.*, **55**, 1081–1088.

Gille, J. C., and J. J. Barnett, 1992: The high resolution dynamics limb sounder (HIRDLS). An instrument for the study of global change, in "The Use of EOS for Studies of Atmospheric Physics," J. C. Gille and G. Visconti, editors, 433–450.

Grainger, R. G., A. Lambert, F. W. Taylor, J. J. Remedios, C. D. Rodgers, M. Corney, and B. J. Kerridge, 1993: Infrared absorption by volcanic stratospheric aerosols observed by ISAMS. *Geophy. Res. Lett.*, **20**, 1283–1286.

Gunson, M. R., et al., Increase in levels of stratospheric chlorine and fluorine loading between 1985 and 1992, 1994: *Geophys. Res. Lett.*, **21**, 2223-2226.

Hanson, D. R., A. R. Ravishankara, and S. Solomon, 1994: Heterogeneous reactions in sulfuric acid aerosols: A framework for model calculations. *J. Geophy. Res.*, **99**, 3615–3629.

Hofmann, D. J., J. W. Harder, J. M. Rosen, J. V. Hereford, and J. R. Carpenter, 1989: Ozone profile measurements at McMurdo Station, Antarctica, during the spring of 1987. *J. Geophys. Res.*, **94**, 16,527–16,536.

Hofmann, D. J., S. J. Oltmans, J. A. Lathrop, J. M. Harris, and H. Vomel, 1994: Record low ozone at the south pole in spring. *Geophys. Res. Lett.*, **21**, 421-424.

Hollandswarth, S. M., R. D. McPeters, L. E. Flynn, W. Planet, A. J. Miller, and S. Chandra, 1995: Ozone trends deduced from combined Nimbus 7 SBUV and NOAA 11 SBUV/2 data. *Geophys. Res. Lett.*, **22**, 905–908.

Holton, J. R., P. H. Haynes, M. E. McIntyre, A. R. Douglass, R. B. Rood, and L. Pfister, 1995: Stratosphere-troposphere exchange. *Reviews of Geophys.*, **33**, 403-439.

Hood, L. L., and J. P. McCormack, 1992: "Components of interannual ozone change based on NIMBUS 7 TOMS data." *Geophys. Res. Lett.*, **19**, 2309–2312.

Huang, T. Y. W., and G. P. Brasseur, 1993: Effect of long-term solar variability in a two-dimensional interactive model of the middle atmosphere. *J. Geophys. Res.*, **98**, 20,413–20,427.

IPCC, "Climate Change, 1994," 1995: (J. Houghton, L. Filho, J. Bruce, H. Lee, B. Callander, E. Haites, N. Harris, and K. Maskell, Eds.) Cambridge University Press, Cambridge, U.K., 339 pp.

IPO, Integrated Operational Requirements Document (IORD) I, March, 1996 IPO, Technical Requirements Document (TRD), Appendix D, NPOESS System EDR Requirements, June, 1998.

Jackman, C. H., J. E. Nielsen, D. J. Allen, M. C. Cerniglia, R. D. McPeters, A. R. Douglass, and R. B. Rood, 1993: The effects of the October 1989 solar proton events on the stratosphere as computed using a three-dimensional model. *Geophys. Res. Lett.*, **20**, 459–462.

Jackman, C. H., M. C. Cerniglia, J. E. Nielsen, D. J. Allen, J. M. Zawodny, R. D. McPeters, A. R. Douglass, J. E. Rosenfield, and R. B. Rood, 1995: Two-dimensional and three-dimensional model simulations, measurements, and interpretation of the influence of the October 1989 solar proton events on the middle atmosphere. *J. Geophys. Res.*, **100**, 11,641–11,660.

Jensen, E. J., O. B. Toon, J. D. Spinhirne, and H. B. Selkirk, 1997: On the formation and persistence of subvisible cirrus clouds near the tropical tropopause, *J. Geophys. Res.*, in press.

Kinnison, D. E., H. S. Johnston, and D. J. Wuebbles, 1994a: Model study of atmospheric transport using carbon 14 and strontium 90 as inert tracers. *J. Geophys. Res.*, **99**, 20,647–20,664.

Kinnison, D. E., K. E. Grant, P. S. Connell, D. A. Rotman, and D. J. Wuebbles, 1994b: The chemical and radiative effects of the Mount Pinatubo eruption. *J. Geophys. Res.*, **99**, 25,705–25,731.

Lefevre, F., G. P. Brasseur, I. Folkins, A. K. Smith, and P. Simon, 1994: Chemistry of the 1991-1992 stratospheric winter: three dimensional model simulations. *J. Geophys. Res.*, **99**, 8183–8197.

Logan, J. A., 1994: Trends in the vertical distribution of ozone: An analysis of ozonesonde data. *J. Geophys. Res.*, **99**, 25,553–25,585.

Mankin, W. G., and M. T. Coffey, 1984: Increased stratospheric hydrogen chloride in the El Chichon cloud, *Nature*, **226**, 170-174.

Mankin, W. G., M. T. Coffey, and A. Goldman, Airborne observations of SO_2, HCl, and O_3 in the stratospheric plume of the Pinatubo volcano in July 1991. *J. Geophys. Res.*, **100**, 2953-2972.

Manney, G.L., L. Froidevaux, M.L. Santee, R.W. Zurek, and J.W. Waters, 1997: MLS observations of the Arctic ozone loss in 1996-1997. *Geophys. Res. Lett.*, **24**, 2697-2700.

Manney, G. L., L. Froidevaux, J. W. Waters, and R. W. Zurek, 1995: Evolution of microwave limb sounder ozone and the polar vortex during winter. *J. Geophys. Res.*, **100**, 2953–2972.

Massie, S. T., P. L. Bailey, J. C. Gille, E. C. Lee, J. L. Mergenthaler, A. E. Roche, J. B. Kumer, E. F. Fishbein, J. W. Waters, and W. A. Lahoz, 1994: Spectral signatures of polar stratospheric clouds and sulfate aerosol. *J. Atmos. Sci.*, **51**, 3027–3044.

McCormick, M. P., and J. C. Larsen, 1988: Antarctic measurements of ozone by SAGE II in the spring of 1985, 1986, and 1987. *Geophys. Res. Lett.*, **15**, 906–910.

McCormick, M. P., L. W. Thomason, and C. R. Trepte, 1995: Atmospheric effects of the Mt. Pinatubo eruption. *Nature*, **373**, 399–404.

McElroy, M. B., R. J. Salawitch, and S. C. Wofsy, 1986: Antarctic O_3: Chemical mechanisms for the spring decrease. *Geophys. Res. Lett.*, **13**, 1296–1297.

Murphy, D., and G. B. Gary, 1995: Mesoscale temperature fluctuations and polar stratospheric clouds. *J. Atmos. Sci.*, **52**, 1753–1760.

Nash, J., and F. Schmidlin, 1987: Final report of the WMO international radiosonde intercomparisons, WMO Report No. 30.

National Plan for Stratospheric Monitoring 1988–1997, 1989: Dept. of Commerce/NOAA, FCM-P17-1989.

Newman, P.A., J.F. Gleason, R.D. McPeters, and R.S. Stolarski, 1997: Anomalously low ozone over the Arctic. *Geophys. Res. Lett.*, **24**, 2689- 2692.

Oberbeck, V. R., J. M. Livingston, P. B. Russell, R. F. Pueschel, J. N. Rosen, M. T. Osborn, M. A. Kritz, K. G. Snetsinger, and G. V. Ferry, 1989: SAGE II aerosol validation: Selected altitude measurements, including particle micromeasurements. *J. Geophys. Res.*, **94**, 8367–8380.

Osborn, M. T., J. M. Rosen, M. P. McCormick, P.-H. Wang, J. M. Livingston, and T. J. Swissler, 1989: SAGE II aerosol correlative observations: Profile measurements. *J. Geophys. Res.*, **94**, 8353–8366.

Pitari, G., V. Rizi, L. Ricciardulli, and G. Visconti, 1993: High speed civil transport impact: Role of sulfate, nitric acid trihydrate and ice aerosols studied with a two-dimensional model including aerosol physics. *J. Geophys. Res.*, **98**, 23,141–23,164.

Pollack, J. B., F. C. Witteborn, K. O'Brien, and B. Flynn, 1991: A determination of the infrared optical depth of the El Chichón volcanic cloud. *J. Geophys. Res.*, **97**, 3115–3122.

Poole, L. R., and M. C. Pitts, 1994: Polar stratospheric cloud climatology based on Stratospheric Aerosol Measurement II observations from 1978-1989. *J. Geophys. Res.*, **99**, 13,083–13,089.

Proffitt, M. H., J. A. Powell, A. F. Tuck, D. W. Fahey, K. K. Kelly, A. J. Drueger, M. R. Schoeberl, B. L. Gary, J. J. Margitan, K. R. Chan, M. Loewenstein, and J. R. Podolske, 1989: A chemical definition of the boundary of the Antarctic ozone hole. *J. Geophys. Res.*, **94**, 11,437–11,448.

Randel, W. J., and J. B. Cobb, 1994: Coherent variations of monthly mean total ozone and lower stratospheric temperature. *J. Geophys. Res.*, **99**, 5433–5448.

Rasch, P. J., B. A. Boville, and G. P. Brasseur, 1995: A three-dimensional general circulation model with coupled chemistry for the middle atmosphere. *J. Geophys. Res.*, **100**, 9041–9071.

Reid, G. C., S. Solomon, and R. R. Garcia, 1991: Response of the middle atmosphere to the solar proton events of August-December 1989. *Geophys. Res. Lett.*, **18**, 1019–1022.

Reinsel, G. C., G. C. Tiao, D. J. Wuebbles, J. B. Kerr, A. J. Miller, R. M. Nagatani, L. Bishop, and L. H. Ying, 1994: Seasonal trend analysis of published ground-based and TOMS total ozone data through 1991. *J. Geophys. Res.*, **99**, 5449–5464.

Report of the International Ozone Trends Panel 1988. 1990: WMO Report 18.

Rinsland, C. P., G. K. Yue, M. R. Gunson, R. Zander, and M. C. Abrams, 1994: Mid-infrared extinction by sulfate aerosols from the Mt. Pinatubo eruption. *J. Quant. Spectrosc. Radiat. Transfer*, **52**, 241–252.

Rood, R. B., A. R. Douglass, J. A. Kaye, M. A. Geller, Y. Chi, D. J. Allen, E. M. Larson, E. R. Nash, and J. E. Nielsen, 1991: Three-dimensional simulations of wintertime ozone variability in the lower stratosphere. *J. Geophys. Res.*, **96**, 5055–5071.

Rottman, G. J., T. N. Woods, and T. P. Sparn, 1993: Solar Stellar Irradiance Comparison Experiment 1: 1. Instrument design and operation. *J. Geophys. Res.*, **98**, 10,667–10,678.

Russell, J. M., M. Luo, R. J. Cicerone, and L. E. Deaver, 1996: Satellite confirmation of the dominance of chlorofluorocarbons in the global stratospheric chlorine budget. *Nature*, **379**, 526–529.

Santee, M.L., G.L. Manney, L. Froidevaux, R.W. Zurek, and J.W. Waters, 1997: MLS Observations of ClO and HNO_3 in the 1996-1997 Arctic polar vortex. *Geophys. Res. Lett.*, **24**, 2713-2716.

Schauffler, S. M., L. E. Heidt, W. H. Pollack, T. M. Gilpin, J. F. Vedder, S. Solomon, R. A. Lueb, and E. L. Atlas, 1993: Measurements of halogenated organic compounds near the tropical tropopause, *Geophys. Res. Lett.*, **20**, 2567-2570.

Schoeberl, M. R., et al., 1993: The evolution of ClO and NO along air parcel trajectories. *Geophys. Res. Lett.*, **20**, 2511–1514.

Solomon, S., 1990: Progress towards a quantitative understanding of the Antarctic ozone depletion. *Nature*, **347**, 347-354.

Solomon, S., R. R. Garcia, F. S. Rowland, and D. J. Wuebbles, 1986: On the depletion of Antarctic ozone. *Nature*, **321**, 755–758.

Solomon, S., R. W. Portmann, R. R. Garcia, L. W. Thomason, L. Poole, and M. P. McCormick, 1996: The role of aerosol variations in anthropogenic ozone depletion at northern midlatitudes. *J. Geophys. Res.*, **101**, 6713–6727.

Sparling, L., et al., 1995: Trajectory modeling of emissions from lower stratospheric aircraft. *J. Geophys. Res.*, **100**, 1427–1438.

Stolarski, R. S., A. J. Drueger, M. R. Schoeberl, R. D. McPeters, P. A. Newman, and J. C. Alpert, 1986: Nimbus 7 satellite measurements of the springtime Antarctic ozone decrease. *Nature*, **322**, 808–811.

Stolarski, R. S., P. Bloomfield, R. D. McPeters, and J. R. Herman, 1991: Total ozone trends deduced from Nimbus 7 TOMS data. *Geophys. Res. Lett.*, **18**, 1015–1018.

Tie, X. X., G. P. Brasseur, and C. Granier, 1994: Two-dimensional simulation of Pinatubo aerosol and its effect on stratospheric ozone. *J. Geophys. Res.*, **99**, 20,545–20,562.

Toon, O. B., P. Hamill, R. P. Turco, and J. Pinto, 1986: Condensation of HNO_3 and HCl in the winter polar stratosphere. *Geophys. Res. Lett.*, **13**, 1284–1287.

Toon, O. B., and M. Tolbert, 1995: Spectroscopic evidence against nitric acid trihydrate in polar stratospheric clouds. *Nature*, **375**, 218–221.

Wallace, L., and W. Livingston, 1992: The effect of the Pinatubo cloud on hydrogen chloride and hydrogen fluoride, *Geophys. Res. Lett.*, **19**, 1209.

Waters, J. W., L. Froidevaux, W. G. Read, G. L. Manney, L. S. Elson, D. A. Flower, R. F. Jarnot, and R. S. Harwood, 1993: Stratospheric ClO and ozone from the microwave limb sounder on the upper atmosphere research satellite. *Nature*, **362**, 597–602.

Weisenstein, D. K., M. K. W. Ko, J. M. Rodriguez, and N. D. Sze, 1993: Effects on stratospheric ozone from high-speed civil transport: Sensitivity to stratospheric aerosol loading. *J. Geophys. Res.*, **98**, 23,133–23,140.

Willson, R. C., and H. S. Hudson, 1991: "A solar cycle of measured and modeled total irradiance." *Nature*, **351**, 42–44.

World Meteorological Organization (WMO), 1992: Scientific assessment of ozone depletion: 1991, Global Ozone Res. and Monit. Proj., World Meteorol. Org., Rep. 25.

World Meteorological Organization (WMO), 1995: Scientific assessment of ozone depletion: 1994, Global Ozone Res. and Monit. Proj., World Meteorol. Org., Rep. 37.

Zander, R., M. R. Gunson, C. B. Farmer, C. P. Rinsland, F. W. Irion, and E. Mahieu, 1992: The 1985 chlorine and fluorine inventories in the stratosphere based upon ATMOS observations at 30 N latitude. *J. Atm. Chem.*, **15**, 171-186.

Chapter 7 Index